

DD-A093 376

KENT UNIV CANTERBURY (ENGLAND)
AN INVESTIGATION OF FAST ION TRANSPORT IN SOLIDS USING CONDUCTI--ETC(U)
OCT 80 A V CHADWICK, D S HOPE, G JAROSKIEWICZ AFOSR-77-3427

F/G 7/4

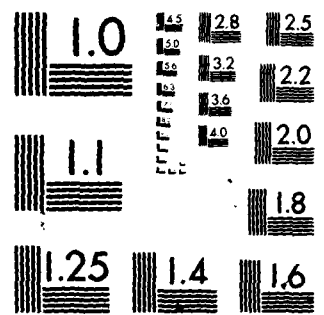
AFOSR-TR-80-1337

NL

BINCLASIFIED

401
3-987

END
DATE
FILED
12-84
DTIC



MICROCOPY RESOLUTION TEST CHART
NATIONAL BUREAU OF STANDARDS-1963-A

AD A093376

Unclassified

LEVEL II

2

REPORT DOCUMENTATION		READ INSTRUCTIONS BEFORE COMPLETING FORM
1. Report Number <i>AFOSR-TR-81-1337</i>	2. Govt Accession No. <i>AD-A093 376</i>	3. Recipient's Catalog Number
4. Title (and Subtitle) <i>AN INVESTIGATION OF FAST ION TRANSPORT IN SOLIDS USING CONDUCTIVITY AND N.M.R. (Fast ion Transport in Solids)</i>	5. Type of Report & Period Covered <i>Final 15 September 1977 to 14 Sept 1980.</i>	6. Performing Org. Report Number
7. Author(s) <i>Alan V. Chadwick, David S. Hope, George Jaroskiewicz and John H. Strange</i>	8. Contract or Grant Number <i>AFOSR-77-3427 new</i>	9. Performing Organization Name and Address <i>Chemistry Laboratory/Physics Laboratory, University of Kent, Canterbury, Kent CT2 7NH, 387267 (ENGLAND)</i>
11. Controlling Office Name and Address <i>Air Force Office of Scientific Research/ Bolling AFB, NC Washington DC 20332</i>	12. Report Date <i>15 October 1980</i>	10. Program Element, Project, Task Area & Work Unit Numbers <i>61102F 2303/A1</i>
14. Monitoring Agency Name and Address	13. Number of Pages <i>89</i>	15. <i>DTIC ELECTE JAN 02 1981</i> Unclassified
16. & 17. Distribution Statement <i>Approved for public release; distribution unlimited.</i>		
18. Supplementary Notes		
19. Key Words <i>Lanthanide Fluorides, Fast Ion Conductors, Ionic Conductivity, N.M.R., Point Defect Structures.</i>		
20. Abstract <i>The lanthanide fluorides and mixtures of these fluorides exhibit fast ion conduction. A study has been made of ionic transport in single crystals of LaF₃ systems using electrical conductivity and N.M.R. techniques. Analysing the conductivity results in terms of Schottky disorder yield values of the defect formation and migration enthalpies as 2.12 and 0.28 eV, respectively. At low temperatures the study of oriented crystals showed the conductivity // to the c-axis was twice that 1 to the c-axis. The N.M.R. relaxation times T₁, T₁₀ and T₂ exhibited a complex behaviour. A model was developed to interpret these results on the basis of non-equivalent F⁻ sites in the lattice. Single crystals of La_{1-x} Sr_x F_{3-x} are good F⁻ ion conductors, better than would have been expected from previous publications. A full discussion of the results has been presented, along with suggestions for future work.</i>		

UNCLASSIFIED

FILE COPY

112 DEC 1980

(18) (19) (15) Contract/Grant Number: AFOSR-77-3427 | (16) 2303 | (17) A11

(6) AN INVESTIGATION OF FAST ION TRANSPORT
IN SOLIDS USING CONDUCTIVITY AND N.M.R.

(Fast ion transport in solids)

(10) Alan V. Chadwick David S. Hope George Jaroskiewicz
John H. Strange
Chemistry Laboratory/Physics Laboratory,
University of Kent,
Canterbury, Kent.
ENGLAND.

(11) 15 Oct 80

(12) 90

(7) Final Report, 15th Sep 77—14th Sep 80,

Approved for public release; distribution unlimited

Prepared for

AFOSR, Bolling AFB, DC 20332

and

European Office of Aerospace Research and Development,
London,
ENGLAND.

Approved for public release;
distribution unlimited.

387367
80 12 29 04 R-NY

CONTENTSPREFACE

	<u>PAGE</u>
I. <u>INTRODUCTION</u>	
I.1. General background	1
I.2. Objectives of the present investigation	7
I.3. Ionic conductivity theory	10
I.4. N.M.R. relaxation theory	18
I.5. Conductivity - N.M.R. approach to the study of diffusion mechanisms	23
II. <u>EXPERIMENTAL</u>	
II.1. Raw materials	24
II.2. Crystal growth	25
II.3. Conductivity measurements	28
II.4. N.M.R. measurements	33
III. <u>RESULTS</u>	
III.1. Sample quality	39
III.2. Conductivity results	40
III.2A. Nominally pure LaF ₃	44
III.2B. Oriented LaF ₃	49
III.2C. Sr ²⁺ doped LaF ₃	51
III.2D. Th ⁴⁺ doped LaF ₃	53
III.3. N.M.R. results	55
III.3A. YF ₃	55
III.3B. LaF ₃	57
IV. <u>DISCUSSION</u>	
IV.1. Comparison of the present results with other transport data for LaF ₃	67
IV.1A. Conductivity data	67
IV.1B. N.M.R. data	72
IV.2. Comparison of the conductivity and N.M.R. data	73
IV.3. The point defect structure and transport mechanisms in LaF ₃	75

Accession For	
NTIS GRA&I	<input type="checkbox"/>
DTIC TAB	<input type="checkbox"/>
Unannounced	<input type="checkbox"/>
Justification	
By _____	
Distribution/ _____	
Availability Codes	
Dist	Avail and/or Special
A	

Contents (Contd.)

	<u>Page</u>
V. <u>CONCLUSIONS</u>	79
VI. <u>RECOMMENDATIONS FOR FUTURE WORK</u>	80
VII. <u>PUBLICATIONS FROM THIS PROJECT</u>	81
VIII. <u>REFERENCES</u>	82

AIR FORCE OFFICE OF SCIENTIFIC RESEARCH (AFSC)
NOTICE OF TRANSMITTAL TO DDC
This technical report has been reviewed and is
approved for public release IAW AFR 190-12 (7b).
Distribution is unlimited.
A. D. BLOSH
Technical Information Officer

PREFACE

Solids which exhibit high ionic conductivities have a number of possible important applications in technological systems e.g. solid state batteries, fuel cells etc. As a consequence the investigation of these materials, which are termed "solid electrolytes" or "fast-ion conductors" or "superionic conductors", is currently one of the most active areas of scientific research. This report describes the work performed in a three year project involved with the study of fast ion conduction in lanthanide fluorides and related materials. The study was aimed at the evaluation of the parameters affecting the ion transport with a view to understanding how they might be controlled with a view to the design of materials with optimum properties.

The research performed in each of the first two years of this project have been reported in individual reports. This report covers the work of the whole three year period of the project. This report is sufficiently self-contained that a detailed reading of our previous reports is not a pre-requisite.

We would like to thank the members of the various technical workshops at the University of Kent for the considerable assistance throughout the course of this project.

Finally we wish to thank Mrs. Diane Devon and Mrs. Beverly Wells for their patience and diligence in the preparation of this report.

I. INTRODUCTION

I.1. General Background

There is an extensive literature, which dates back to the beginning of this century, describing the possible uses of solid ionic conductors in devices. The early electrochemists were aware of the potential use of solid electrolytes in galvanic cells for energy conversion. More recent applications for these materials include solid state batteries, fuel cells, thermoelectrochemical cells, electrochromic displays, electrochemical integrators, coulometers and discrete components. However the majority of the proposals for solid electrolytes never reached fruition in terms of a commercial device. The dominant reason for this was that nearly all the known ionic materials were very poor electrical conductors at ambient temperatures. In the 1960's there was a revival of interest in solid electrolytes. There are a number of reasons for the re-opening of this area of research and they include the development of highly conducting materials, such as $A\text{Ag}_4\text{I}_5$ (where A is an alkali metal or NH_4^+) and β -alumina, the use of solid state electrolytes in fuel cells, in particular stabilized zirconia, and the development of the high energy density sodium/sodium- β -alumina/sulphur battery. Currently there is an intense research effort into all aspects of highly conducting solids, which are now termed "fast ion conductors" or "superionic conductors" or "solid electrolytes". A measure of this interest can be gauged by the large number of papers and reviews⁽¹⁻⁷⁾ that have been published and the number of conferences

-
- (1) McGeehin, P. and Hooper,A., 1975, "Fast ion conduction: A materials review", Harwell report, AERE-R8070.
 - (2) Van Gool, W., 1973, (ed) "Fast ion transport in solids", (North-Holland, Amsterdam).

that have been devoted to fast ion conductors⁽⁸⁻¹¹⁾.

Research into fast ion conduction can be broadly divided into three areas; the development of a basic understanding of the phenomenon, the search for new materials and the production of commercial devices. The most general coverage of all three areas was given at the Lake Geneva Conference⁽¹⁰⁾. The production of some commercial devices is now in progress. The sodium-sulphur battery based on a sodium- β -alumina electrolyte is now reputedly beyond the prototype stage. In the next few years these should be commercially available and the proposed uses include load-levelling and vehicular traction. Small batteries

-
- (3) Huggins, R., 1975, in "*Diffusion in solids - recent developments*", ed. Nowick and Burton (Academic Press, New York), chapter 9, p.445.
 - (4) Hooper, A., 1978, *Contemp. Phys.*, 19, 147.
 - (5) Hagenmuller, P. and van Gool, W., 1978, ed. "*Solid Electrolytes; General principles, characterization, materials, applications*" (Academic, New York).
 - (6) Geller, S., 1977, ed. "*Solid Electrolytes*" Topics in Applied Physics, Volume 21 (Springer, Berlin).
 - (7) Salamon, M.B., 1979, ed. "*Physics of Superionic Conductors*" Topics in Current Physics, Volume 15 (Springer, Berlin).
 - (8) Mahan, G.D. and Roth, W.L., 1976, ed. "*Proc. Int. Conf. on Fast Ion Conductors, Schenectady*", (Plenum, New York).
 - (9) Second International Conference on Solid Electrolytes, 7-21 September 1978, St. Andrews, Scotland (no published proceedings).
 - (10) Vashista, P., Mundy, J.N. and Shenoy, G.K., 1979, ed. "*Fast Ion Transport in Solids*", (North-Holland, New York). Proceedings of International Conference held 21-25 May 1979 at Lake Geneva, Wisconsin, U.S.A.
 - (11) Third International Conference on Solid Electrolytes, September 1980, Tokyo, Japan.

based on silver containing solid electrolytes are already in use in the medical field⁽¹²⁾. A very wide range of materials is being investigated in the search for potential fast ion conductors. These include glasses⁽¹³⁾ and "loaded" polymers⁽¹⁴⁾ in addition to crystalline materials. Particularly useful materials would be fast ion conductors based on ions of elements with a high natural abundance (Na, K, Cu, Li, halogens) and protons.

The principal features of fast ion conductors have been summarized in a number of reviews⁽¹⁾ and can be listed as follows:-

- (i) a large number of mobile ions;
- (ii) a large number of available sites, per mobile ion, i.e. materials with a high concentration of point defects;
- (iii) a low activation energy for ion migration;
- (iv) structures with continuous "tunnels" through which the mobile ions can diffuse.

A consequence of feature (ii) is that the theories of conductivity used so successfully in the interpretation of simple ionic crystals⁽¹⁵⁾, like the alkali halides, which have low defect concentrations, i.e. <<1%>> are not applicable to fast ion conductors. For example, sophisticated treatments would be required to handle the effect of defect-defect interactions on the defect concentrations and the defect mobility.

(12) Owens, B.B., Oxley, J.E. and Sammells, A.F., 1977, in "Solid Electrolytes" ed. Geller (Springer, Berlin).

(13) See articles in reference (10).

(14) Armand, M.B., Chabagno, J.M. and Duclot, M.J., 1979, in "Fast Ion Transport in Solids" ed. Vashishta, Mundy and Shenoy (North-Holland, New York) p.131.

(15) Lidiard, A.B., 1957, in "Handbuch der Physik", Volume XX ed. Flügge (Springer, Berlin), p.246.

The earliest treatments⁽²⁾ of fast ion conduction were based on treating the mobile ion sub-lattice as being "liquid-like". Although this has proved a qualitatively useful approach it has not got quantitative applications. Other theoretical approaches that have been proposed include a "free-ion" model⁽¹⁶⁾ and the path probability method⁽¹⁷⁾. The approach that does seem to be valuable is that of molecular dynamics simulation and there has been a growing number of papers using this technique.⁽¹⁸⁻²⁰⁾ However, a detailed understanding of the phenomenon is not yet possible even in the simplest systems that have been studied and there are many questions which have yet to be answered. The peculiarites of fast-ion conduction are nicely reviewed by Salamon⁽⁷⁾. He points out the difficulties in trying to modify existing solid state theories to treat fast ion conduction and the need for new approaches.

In addition to the theoretical problems in treating fast ion conductors there are also a number of experimental problems. Many fast ion conductors are not suited to the precise measurements which can be made for normal ionic crystals. For example, the data for non-stoichiometric fast ion conductors strongly depend upon composition. Some materials, like the β -alumina, are not readily available in the form of well-characterised single crystals and this precludes many types of informative experiment. Other materials, particularly those

(16) Rice, M.J., 1973, in "*Fast ion transport in solids*", ed. van Gool (North-Holland, Amsterdam), p.263 and references therein.

(17) Sato, H. and Kikuchi, R., 1971, J.Chem.Phys., 55, 677 and 702.

(18) Jaccucci, G. and Rahman, A., 1978, J.Chem.Phys., 69, 4117.

(19) Dixon, M. and Gillan, M.J., 1980, J.Phys.C: Solid State Phys. 13, 1901 and 1919.

(20) De Leeuw, S.W., 1978, Molec.Phys., 36, 103.

containing silver or fluorine, are highly reactive and great care is necessary to avoid sample contamination.

A number of groups, including ourselves, have taken the view that good progress in the understanding of fast ion conduction could be made by a careful study of simple materials which exhibit this behaviour. With this in mind we undertook studies of fluorite materials. In particular we used the combination of ionic conductivity and N.M.R. relaxation time measurements in order to try to determine the diffusion mechanisms operative in these systems in both their low temperature⁽²¹⁾ and fast conducting phases^(22,23). This work proved to be extremely successful from the experimental viewpoint; a number of techniques were developed for materials preparation, electrical measurements and the improvement of the N.M.R. techniques. The mechanism of conduction in the fast ion conducting phase of fluorites is still not understood^(24,25). However, we believe that we have made a significant contribution to this field and it encouraged us to extend the work to the present investigation of rare earth fluorides.

When the project was initiated there had been only a few studies of transport in rare earth fluorides. There had been conductivity⁽²⁶⁻²⁸⁾

-
- (21) Figueroa, D.R., Chadwick, A.V. and Strange, J.H., 1978, J.Phys.C: Solid State Phys., 11, 55.
 - (22) Carr, V.M., Chadwick, A.V. and Saghafian, R., 1978, J.Phys.C: Solid State Phys., 11, L637.
 - (23) Gordon, R.E. and Strange, J.H., 1978, J.Phys.C: Solid State Phys., 11, 3218.
 - (24) Catlow, C.R.A., 1980, Comments in Solid State Phys. (in press).
 - (25) Schoonman, J., 1980, Solid State Ionics, 1, 121.
 - (26) Sher, A., Solomon, R., Lee, K. and Muller, M.W., 1966, Phys.Rev., 144, 593.
 - (27) Fielder, W.L., 1969, NASA Technical Report D-5505.

and N.M.R. (26, 29, 30) measurements of transport in LaF_3 . A study of conductivity in CeF_3 had also been reported⁽³¹⁾. These works were interesting in that they showed that the (1) mobile ion was the fluoride ion, (ii) the conductivity was in the range for these materials to be classed as fast ion conductors and (iii) it could be significantly increased by doping with aliovalent impurities. Thus these materials have potential applications in systems where fast F^- conduction is required⁽³²⁾ and merited further investigation. In addition, these materials are structurally relatively simple and are useful models for basic investigations of fast ion conduction. They can also be prepared as large single crystals and are easily doped which is a real asset in experimental investigations of transport. For these reasons we chose the rare earth fluorides and some related materials as the subject of this project.

-
- (28) Nagle, L.E. and O'Keefe, M., 1973, in "*Fast ion transport in solids*", ed. van Gool (North-Holland, Amsterdam) p.165.
 - (29) Goldman, M. and Shen, L., 1966, Phys.Rev., 144, 321.
 - (30) Lee, K. and Sher, A., 1965, Phys.Rev.Letters, 14, 1027.
 - (31) Takahashi, T., Iwahara, H. and Ishikawa, T., 1977, J. Electrochem.Soc., 124, 208.
 - (32) Reau, J-M. and Portier, J., 1978, "*Solid Electrolytes*" ed. Hagenmuller and van Gool (Academic, New York) p.313.

1.2 Objectives of the present investigation

Previous work has shown that the rare earth fluorides and some of their mixtures with other fluorides exhibit fast F⁻ ion conduction and could be useful in devices. However, that work did not provide the precise information that is required to provide accurate defect energies and of the type that could be used to test theories of fast ion conduction. Many of these fluorides have been grown as good single crystals and are structurally simple or interesting. Thus a thorough investigation of these systems will help the understanding of fast ion conduction and provide a quantitative basis for the design of F⁻ ion conductors. It was on this basis that we began our ambitious three-year project on these materials.

We chose three types of fluoride in which to study transport by the combined conductivity - N.M.R. approach. These are as follows:-

(a) Rare earth fluorides (LnF₃)

At elevated temperatures these materials can be classed as fast F⁻ ion conductors⁽²⁶⁻³¹⁾. LaF₃, CeF₃, PrF₃, NdF₃ and PmF₃ all have the hexagonal tysonite LaF₃ structure⁽³³⁾ which is shown in Figure 1. These materials have been grown as good single crystals. YF₃ and the heavier rare earths fluorides are dimorphic; the room temperature form has an orthorhombic structure and there is a transition to the LaF₃ structure at high temperatures. Large crystals of the room temperature form have not been grown. LaF₃ and YF₃ were chosen for study. Other rare earth fluorides, with the exception of LuF₃, would not be suitable for N.M.R. diffusion studies since their La³⁺ ion is paramagnetic.

(33) Brown, D., 1968, "Halides of the Lanthanides and Actinides", (Wiley-Interscience, London).

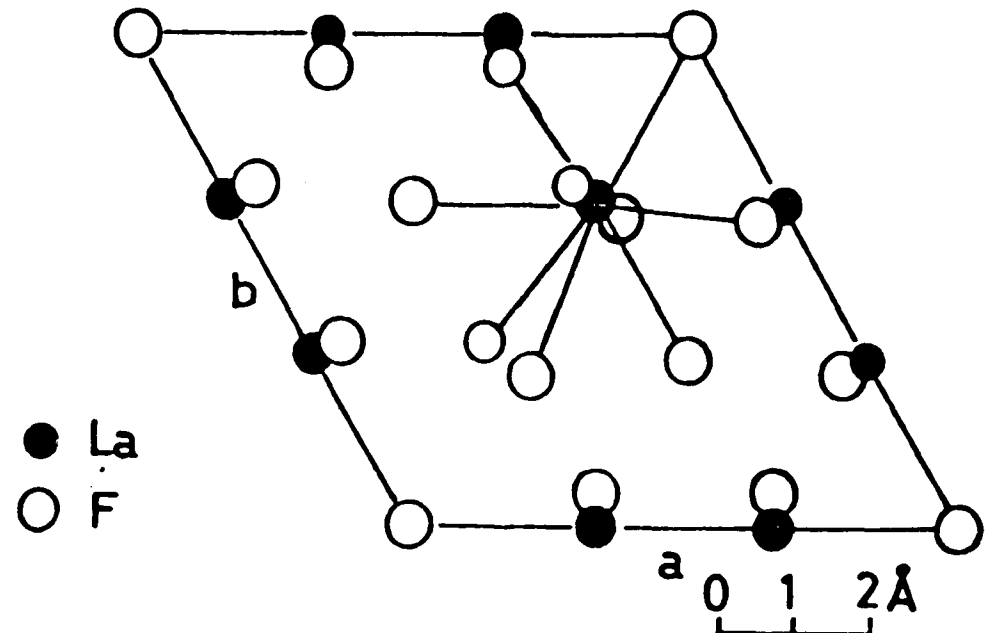


FIGURE 1

THE NINEFOLD COORDINATION OF LANTHANUM IN LANTHANUM TRIFLUORIDE AS VIEWED DOWN THE C AXIS (AFTER ZALKIN ET AL., REF 43.)

(b) Tysonite - related fluorides ($\text{Ln}_{1-x} \text{B}_x \text{F}_{3-x}$)

- where B is an alkaline earth ion.

The few systems that have been studied show extremely high conductivities (e.g. $\text{La}_{0.95} \text{Sr}_{0.05} \text{F}_{2.95}$ has a conductivity of 10^{-4} ohm $^{-1}$ cm $^{-1}$ at room temperature⁽²⁸⁾). These were chosen for study, and of particular interest is the relationship between conductivity and composition.

(c) Mixed fluorides (ALn F_3)

- where A is an alkali ion.

The structure of these materials depends on A and Ln. Of particular interest are the materials like KLa F_4 which have a low temperature hexagonal scheelite structure which transform to a cubic fluorite structure at high temperatures. In these compounds F^- is very mobile and there is the possibility that A^+ is mobile⁽³⁴⁾. The current research effort into the fluorites makes these systems additionally attractive.

Our aim was to use our techniques to gain the following information:-

- (i) accurate diffusion parameters for the constituent ions from room temperature to near the melting point;
- (ii) an identification of the mechanisms of diffusion;
- (iii) information on the point defect structure;
- (iv) the relevance of the phase transitions and their effect on ionic transport.

(34) Roth, W.L. and Muller, O., 1974, "Study, selection and preparation of solid cationic conductors". Final report N74-26498 (NASA - CR-134610).

I.3. Ionic conductivity theory

Detailed theoretical treatments of diffusion and electrical conductivity in ionic crystals can be found in several texts^(15,35). These have been developed for simple systems like the alkali halides where the defect concentrations are low. This is not the case for fast ion conductors. However, these treatments do provide a starting basis for the interpretation of the low temperature data in the rare earth fluoride systems and may help reveal the important factors in fast ion conduction. Thus a brief review of the treatments will be given here.

Translational diffusion in an ionic crystal occurs by the action of point defects. For example, an ion can diffuse by exchanging with a vacancy on an adjacent lattice site or the diffusion may be due to the motion of ions on interstitial sites. The transition frequency with which an ion exchanges position with a point defect on a neighbouring site is given by:

$$\omega = \bar{v} \exp(-g_m/RT). \quad (1)$$

Here g_m can be regarded as a free energy of activation, with a corresponding enthalpy, h_m , and entropy, s_m , and \bar{v} is usually taken as the Debye frequency.

If a defect of type j makes Γ_j jumps per unit time (= $\omega_j \times$ the number of equivalent steps) each corresponding to a scalar displacement s_j then the defect diffusion coefficient is given by the Einstein equation:

$$D_j = \left(\frac{1}{6}\right) \Gamma_j s_j^2 \quad (2)$$

In an applied electric field the electrical mobility λ_j (the drift velocity per unit field) of the defect is related to the diffusion

(35) Corish, J. and Jacobs, P.W.M., 1973, in "Surface and defect properties of solids", Vol. II (The Chemical Society, London) p.160.

coefficient by the Nernst-Einstein equation:

$$\frac{\lambda_j}{D_j} = q_j e / kT \quad (3)$$

where $q_j e$ is the virtual charge of the defect. The total ionic conductivity of a crystal is given by the usual relation:

$$\sigma = \sum_j n_j q_j e \lambda_j \quad (4)$$

where n_j is the number of j defects per unit volume. Substituting for λ_j in equation (4) yields

$$\sigma = \left(\frac{e^2}{kT} \right) \sum_j n_j q_j^2 D_j \quad (5)$$

$$\text{and } \sigma = \frac{1}{6} \left(\frac{e^2}{kT} \right) \sum_j n_j q_j^2 r_j s_j^2 \quad (6)$$

For an ion I which is diffusion via a defect j by a single vacancy mechanism the diffusion coefficient is given by the Einstein equation:

$$D_{I,j} = r_{I,j} s_{I,j} / 6. \quad (7)$$

It should be noted the $D_{I,j}$ neglects the effects of correlation motion.

The relationship between defect and ion jump frequencies is:

$$\begin{aligned} r_{I,j} &= m_{I,j} (n_j / N_I) r_j \\ &= m_{I,j} c_j r_j \end{aligned} \quad (8)$$

where $m_{I,j}$ is the number of ions involved in each jump of the defect ($=1$ for vacancy diffusion), N_I is the number of ions per unit volume and c_j is the site fraction of defects (since $N_I \gg n_j$). Thus when conduction is dominated by a single mechanism equations (5) and (6)

can be re-written as:

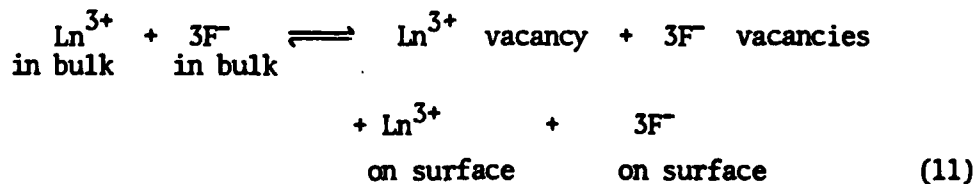
$$\sigma = (N_I q_j^2 e^2 / kT) (D_{I,j} s_j^2 / m_{I,j} s_{I,j}^2) \quad (9)$$

and

$$\sigma = \frac{1}{6} (N_I q_j^2 e^2 / kT) (\Gamma_{I,j} s_j^2 / m_{I,j}). \quad (10)$$

Clearly if an expression can be written down for c_j , which is possible if the defect structure is known for the material, then an explicit expression can be obtained for σ . In our earlier work, given in previous reports, we assumed that LaF_3 contained Schottky disorder and used a simple analysis which could be employed to determine defect enthalpies. This was a standard approach and relied on there being easily identifiable linear regions in the conductivity plot i.e. plots of $\log \sigma T$ against $1/T$. However, a more reliable and useful approach is to develop the full expressions for c_j , and hence σ , and to use computer fitting programmes to analyse the data⁽³⁵⁾. Since we are not at the stage where computer analysis is feasible and useful the more detailed expressions for c_j have to be derived.

The most reasonable assumption is that the predominant point defects in a rare earth fluoride, LnF_3 , Schottky defects, i.e. Ln^{3+} and F^- vacancies. For simplicity we will assume that all the F^- lattice sites are equivalent. Thus defect formation can be described by a quasi-chemical equilibrium⁽¹⁵⁾



If we assume that the number of Ln^{3+} and F^- vacancies are n_{Ln}^V and n_{F}^V ,

respectively, and that N_{Ln} and N_F are the number of Ln^{3+} and F^- ions, respectively, then by statistical thermodynamics it can be shown that

$$\left(\frac{n_F^V}{N_F + n_F^V} \right)^3 \cdot \left(\frac{n_{Ln}^V}{N_{Ln} + n_{Ln}^V} \right) = K_s \quad (12)$$

Here K_s is the equilibrium constant for the quasi-chemical reaction. The terms on the l.h.s. are clearly site fractions*. Thus we can write

$$(c_F^V)^3 \cdot (c_{Ln}^V) = K_s = \exp \left(\frac{-g_s}{kT} \right) \quad (13)$$

where $g_s (=h_s - T\delta_s)$ is the Gibbs Free Energy of formation of the Schottky quartet. It is worth noting that in a pure crystal

$$(N_F + n_F^V) = 3(N_{Ln} + n_{Ln}^V) \quad (14)$$

and

$$n_F^V = 3n_{Ln}^V \quad (15)$$

and

$$c_F^V = c_{Ln}^V \quad (16)$$

We will now assume that the crystal contains a total number of M^{2+} impurity ions given by N_{M2}^T and that these ions dissolve in the lattice substitutionally for Ln^{3+} ions. The M^{2+} ions have virtual negative charges and will tend to associate with defects of opposite virtual charge, i.e. the F^- vacancies. When the M^{2+} ion and F^- vacancy are on nearest neighbour sites they can be regarded as a separate, neutral species(complexes) which will not contribute to the ionic

* Footnote:- In our terminology a site fraction c_j always refers to the ratio of the number of species j and the number of sites which j can occupy.

conductivity. Thus we can consider two forms of M^{2+} ion, "free" M^{2+} ions of number N_{M2}^f , and those in complexes. The number of complexes will be designated n_k .

The doped crystal must be electrically neutral and this condition leads to the relationship

$$3N_{Ln} + 2N_{M2}^T = N_F \quad (17)$$

In addition, there is the condition that the number of cation and anion sites must be equal i.e.

$$3[N_{Ln} + N_{M2}^f + n_{Ln}^v] = N_F + n_F^v + n_k \quad (18)$$

Subtracting (17) from (18) yields

$$3N_{M2}^f + 3n_{Ln}^v + 3n_k - 2N_{M2}^T = n_F^v + n_k \quad (19)$$

and remembering

$$N_{M2}^T = N_{M2}^F + n_k \quad (20)$$

we can write

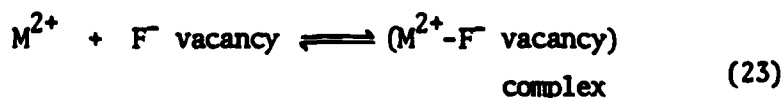
$$N_{M2}^f + n_k + 3n_{Ln}^v = n_F^v + n_k,$$

$$N_{M2}^f + 3n_{Ln}^v = n_F^v \quad (21)$$

[Equation (21) merely shows, as expected, that defect compensation of M^{2+} doping will be the creation of F^- vacancies.] Dividing through equation (21) by N_{Ln} (i.e. provided $N_{M2}^f, n_{Ln}^v, n_k \ll N_{Ln}$, then N_{Ln} can be taken as the number of cation sites) yields

$$c_{M2}^f + 3c_{Ln}^v = 3c_F^v \quad (22)$$

The formation of M^{2+} - F^- vacancy complexes can be represented by the quasi-chemical equilibrium



Using a mass action approach yields

$$\frac{n_k}{n_F^v \cdot N_{M2}^f} = z K_k \\ = z \exp \left(\frac{g_a}{kT} \right) \quad (24)$$

Here K_k is the equilibrium constant for the association and g_a ($= h_a - T s_a$) is the Gibbs Free Energy of association. The numerical factor z is simply the number of possible orientations of the complex. For simplicity we will use

$$K_{ka} = z K_k \quad (25)$$

and converting to site fractions yields

$$\frac{c_k}{c_F^v \cdot c_{M2}^f} = K_{ka} \quad (26)$$

We now have expressions describing the defect equilibria i.e. equations (13), (20), (22) and (26). These can be solved to yield an equation in c_F^v and constants of the form

$$9K_{ka}(c_F^v)^5 + 3(c_F^v)^4 - c_{M2}^T (c_F^v)^3 - 9K_s K_{ka} c_F^v - 3K_s = 0 \quad (27)$$

Since the defect compensation of M^{+} or O^{2-} doping LnF_3 is also by the creation of F^- vacancies then in these cases the equation for c_F^v is analogous to equation (27). A similar derivation has been used to treat the case of M^{4+} doping with compensation by Ln^{3+} vacancies. The combination of equations (10) and (27) gives a complete description of the conductivity as a function of temperature. In total this description involves 9 parameters:-

h_s, s_s (Schottky parameters)

h_a, s_a ($M^{2+}-F^-$ vacancy association parameters)

h_{mF} , s_{mF} (F^- vacancy activation parameters for migration)

h_{mLn} , s_{mLn} (Ln^{3+} vacancy activation parameters for migration)

c_{M2}^T

By the use of an efficient non-linear least-squares programme, such as NLIN2⁽³⁶⁾, conductivity data can be fitted to the above expressions and values of the 9 parameters determined. The procedure is to make initial quesses of the 9 parameters. The value of c_F^V is then obtained by solving equation (27) by the Newton method. The value of c_{Ln}^V is then determined from equation (13). The defect concentrations are then substituted into equation (10) and a conductivity calculated, σ_{calc} . This calculation is performed at each temperature of the experimental data. The difference between σ_{calc} and the experimental conductivity, σ_{expt} is then evaluated and the sum of the deviations squared, \emptyset , is obtained. The programme then goes through a number of interactions, each time adjusting the parameters and repeating the above procedure, until the minimum value of \emptyset is obtained.

There are several advantages in using computer fitting. The major advantage is that all the parameters are determined, entropies and enthalpies, so that defect concentrations, diffusion coefficients, transport numbers etc. can be estimated. It is also a straightforward procedure to build-in the effects of the long-range interaction terms using the Debye-Hückel-Lidiard model and Onsager-Pitts mobility factor⁽³⁵⁾. It could be extended to a more complex model of LnF_3 which would include the non-equivalence of the F^- sites, however, caution would

(36) Marquardt, D.W., 1963, J.Soc.Ind.Appl.Math., 11, 431.

be needed since increasing the number of variable parameters can lead to misleading fits between models and data. The modelling of the non-equivalence of the F⁻ sites in LnF₃ in such a way that can be experimentally tested is still a major problem.

1.4 N.M.R. Relaxation Theory

In a conventional solid the relaxation times T_1 , $T_{1\rho}$, T_2 are related to the spectral densities for atomic motion, $J^Q(\omega)$, in the weak-collision regime, by the dipole-dipole interaction expressions^(37,38):

$$\frac{1}{T_1} = \frac{3}{2} \gamma^4 h^2 I(I+1) \left[J^{(1)}(\omega_0) + J^{(2)}(2\omega_0) \right] \quad (28)$$

$$\frac{1}{T_{1\rho}} = \frac{3}{8} \gamma^4 h^2 I(I+1) \left[J^{(0)}(2\omega_1) + 10J^{(1)}(\omega_0) + J^{(2)}(2\omega_0) \right] \quad (29)$$

$$\frac{1}{T_2} = \frac{3}{8} \gamma^4 h^2 I(I+1) \left[J^{(0)}(0) + 10J^{(1)}(\omega_0) + J^{(2)}(2\omega_0) \right]. \quad (30)$$

For the weak-collision regime $H_0 \gg H_1 \gg H_D$, where H_0 is the constant field (typically several kgauss), H_1 is the rf applied field (typically several tens of gauss) and H_D is the local dipole field of the nuclei in question (a few gauss). The implication of this for most substances is that the experimental behaviour of T_1 , $T_{1\rho}$, T_2 follows the pattern given in Figure 2.

The analysis leading to these equations assumes a single nuclear species relaxing with experimentally observed exponential decays characterised by T_1 , T_2 , or $T_{1\rho}$ (depending on what is being measured). The major theoretical problem usually reduces to the calculation of the spectral functions $J^Q(\omega)$, which can be done in several approximate ways⁽³⁹⁻⁴²⁾. These functions are intimately connected with the atomic hopping motions, and allow determination of jump frequencies for the ions, i.e. $\Gamma_{I,j}$.

(37) Abragam, A., *The Principles of Nuclear Magnetism* (The Clarendon Press, Oxford, England, 1961).

(38) Look, D.C. and Lowe, I.J., 1966, *J. Chem. Phys.*, 44, 2995.

(39) Torrey, H.C., 1953, *Phys. Rev.*, 92, 962.

(40) Eisenstadt, M. and Redfield, A.G., 1963, *Phys. Rev.*, 132, 635.

(41) Sholl, C.A., 1974, *J. Phys. C: Solid St. Phys.*, 7, 3378.
1975, *J. Phys. C: Solid St. Phys.*, 8, 1737.

(42) Wolf, D., 1974, *Phys. Rev.*, 10, 2710.

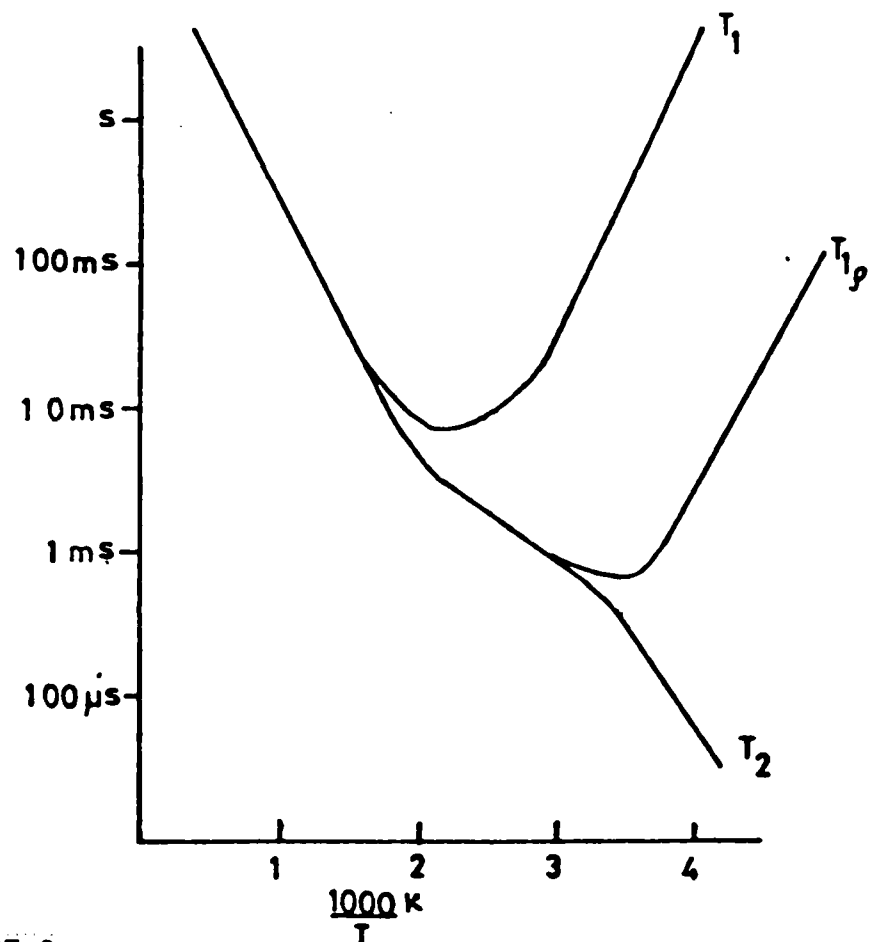


FIGURE 2

TYPICAL N.M.R. RELAXATION TIMES

However, a substance such as LaF_3 really defies such a simple description. The structure of LaF_3 is complex, and for many years there was disagreement about its exact form. Independent observers have now agreed on a heximolecular unit cell based on the group $D_{3d}^4 - P_{\bar{3}Cl}^{(43, 44)}$. Figure 1. It becomes probable on examination of the size of the ions and of the unit cell parameters that interstitial positions for F^- ions are unlikely. In addition, the much greater mass ratio of La to F (7.3 to 1) favours a picture in which the conductivity is produced only by mobile F^- ions that move via vacancy mechanisms. The reported observations that LaF_3 contains Schottky defects supports this view⁽³⁰⁾.

The real problem in studying the N.M.R. of LaF_3 if the probable existence of inequivalent F^- ion sites. What this means is that the crystal can be viewed as three or more sub-lattices superimposed in space. One of these consists of La^{3+} sites, and it is a reasonable assumption to suppose that the La^{3+} ions remain to all intents and purposes fixed on the lattice. The other sublattices are at least two in number, and possibly four. F^- ions situated on these sublattices behave differently, according to which sublattice they are on. In many substances, each lattice point is equivalent to any other, in that the jump probability to a nearest neighbour is the same for all points. For a substance such as LaF_3 this is not so. There are two (at least) sublattices for the F^- ions, labelled A and B. If an F^- ion finds itself on sublattice A, it hops about this sublattice with a relatively fast jump time, whereas if it is on sublattice B it tends to remain fixed, at least at low temperatures. If the drift of F^- ions between these sublattices is small or negligible, then to all intents and purposes there are two distinct F^- species. This is not the same as a

(43) Zalkin, A. et al., 1966, Inorg. Chem., 5, No. 8, 1467.

(44) Mansmann, M., 1964, Z. Anorg. Chem., 331, 98.

chemical shift, i.e. the nuclear g values of these inequivalent F⁻ ions are not changed by different chemical environments at inequivalent lattice sites. This, as well as the existence of two F⁻ species, can be seen in continuous N.M.R. absorption spectra of LaF₃⁽³⁰⁾. Thus the Larmor frequencies for the inequivalent F⁻ ions are identical.

In the region where two distinct F⁻ species can be assumed, it is not correct to assume a single relaxation time. This has important consequences for experimental interpretation. If the F⁻ magnetisations are written as A and B for the two sublattice ensembles of F⁻ ions, then in general we will find the approximate rate equations given by

$$\dot{A} = -\alpha A - \beta B \quad (31)$$

$$\dot{B} = -\gamma A - \delta B , \quad (32)$$

i.e., a cross-relaxation between the two F⁻ species. Since the observed signal is the net F⁻ magnetisation A+B, its decay is not strictly exponential. We find from the above equations

$$(A + B) = (A + B)_{\infty} + Ce^{-\gamma_+ t} + De^{-\gamma_- t} \quad (33)$$

where C, D are constants, and γ_+ , γ_- given by

$$\gamma_{\pm} = \frac{\alpha + \delta \pm \sqrt{(\alpha - \delta)^2 + 4\gamma\beta}}{2} \quad (34)$$

At large enough times, the term in γ_+ will drop out first, and the decay appear approximately exponential, with relaxation time $(\gamma_-)^{-1}$. As Goldman and Shen observed⁽²⁹⁾, accurate measurements of the Free Induction Decay of the F⁻ signal in LaF₃ reveal a non-exponential behaviour just after the initial pulse, followed by an asymptotic exponential decay. In the experiments carried out, the quoted relaxation times are always measured sufficiently far away from the pulse to be exponential relaxation times, i.e. associated with γ_- .

A theory of the functions of temperature α , β , γ , and δ for the N.M.R. relaxation times T_1 , T_2 , $T_{1\rho}$ has now been developed as part of this project. In this theory, a single fluorine species moves over inequivalent sites A and B, so there are three characteristic jump times, viz. $\tau_{A \rightarrow A}$, $\tau_{A \rightarrow B}$, $\tau_{B \rightarrow B}$.

The full theory is too long to present here, and will be submitted for publication elsewhere⁽⁴⁵⁾. It suffices to say that the functions α , β , γ , and δ each consist of two distinct terms. For example,

$$\alpha = \alpha_{DD} + \alpha_E , \quad (35)$$

where α_{DD} is the term due to dipole-dipole interaction, and α_E is the term due to sublattice exchange $A \leftrightarrow A$. The dipole-dipole terms contain many spectral functions $J(\omega)$, the evaluation of which requires full knowledge of the jump probabilities of the fluorines with time. For a single site situation, such as in the cubic-based structures (e.g. the fluorites), the exact treatment of the jump probabilities was satisfactorily solved only fairly recently by Wolf⁽⁴²⁾. In the present case the presence of inequivalent sites makes the problem very much worse. However, if a perturbation in terms of successive jumps is made, then the leading term (which in fact represents the effect of not jumping) dominates, and a reasonable estimate of the spectral functions can be expected. This approximation is of the form given by Torry⁽³⁹⁾, with lattice sums as coefficients, viz.

$$J(\omega) \propto \frac{\sum}{r} \left(\frac{1}{r^6} \right) \frac{\tau}{1+\omega^2\tau^2} \quad (36)$$

The various lattice sums can be evaluated very accurately from the known LaF_3 structure^(43,44), with the consequence that no arbitrary normalisation constants emerge (except for the three jump times mentioned above). Hence the full data for T_1 , T_2 , $T_{1\rho}$ for a given crystal provides a very good test of this theory.

(45) Jarosziewicz, G. and Strange, J.H. (to be published).

I.5. Conductivity - N.M.R. approach to the study of diffusion mechanisms.

From the previous sections it is evident that values of $\Gamma_{I,j}$ and $D_{I,j}$ can be evaluated from both conductivity and N.M.R. relaxation time measurements. However, in both cases the evaluation of these parameters requires the assumption of a specific model for the diffusion mechanism that is operative in the system. What makes the combination of conductivity and N.M.R. a powerful technique in the evaluation of diffusion mechanisms is that they measure the effects of diffusion on different physical properties. Conductivity measures the effect of current flow due to the motion of many ions undergoing a large number of jumps between lattice sites and hence it is a macroscopic property. N.M.R. measures the effect of ionic motion on the local nuclear dipole-dipole interactions and hence monitors a microscopic property. Thus if a specific model of the diffusion mechanism produces the same values of $\Gamma_{I,j}$ and $D_{I,j}$ from both N.M.R. and conductivity data then this is very strong evidence for the validity of the model.

Examples of the use of this procedure can be seen in our studies of BaF_2 (21) and PbF_2 (22,23). An essential experimental point is that in the study of doped systems the same sample must be used in both experiments. It is also important that the temperature scales of the two experiments are carefully checked for consistency. There are obviously complications to be resolved when the crystal structure is not of a high symmetry as would be the case with LnF_3 .

II. EXPERIMENTAL

II.1. Raw Materials

Rare earth fluorides have been obtained from a range of sources:-

- LaF_3 - powder - Koch-Light Ltd.
- LaF_3 - Optran zone-refined pieces - B.D.H. Ltd.
- LaF_3 - high purity lumps - Rare Earth Products Ltd.
- LaF_3 - crystals - Optovac Ltd.
- LaF_3 - crystals - B.D.H. Ltd.
- YF_3 - powder - Koch-Light Ltd.
- YF_3 - high purity lumps - Rare Earth Products Ltd.
- ThF_4 - powder - B.D.H. Ltd.

Other fluorides used to dope crystals have been obtained in the form of B.D.H. Optran grade zone-refined pieces or powder and Harshaw crystal pieces.

The majority of the LaF_3 crystals that we have used have been grown from the Rare Earth Products material.

A sample of LaF_3 powder was prepared by reacting La_2O_3 (high purity, Koch-Light Ltd.) with aqueous HF(B.D.H. Ltd. A.R. grade). The resultant material was dehydrated by mixing it with NH_4Cl and heating to 300°C .

II.2. Crystal growth

The apparatus used was an r.f. induction furnace manufactured by Electroheating Limited (London). It is provided with rotation and lift motors with gear boxes and was originally designed to operate by the Czochralski method. This technique was not found to be convenient for the present work because of the relatively high melting temperatures of the materials. It was consequently decided to employ the Stockbarger method⁽⁴⁶⁾.

The main features of the apparatus are shown in Figure 3. Two end plates carry flat silicon rubber gaskets sealed against a quartz chamber (70 mm bore, 460 mm long). Both plates are water cooled and have parts for vacuum or gas entries. A vertical rod supporting the crucible passes through a long water cooled region of the upper work-chamber plate. The rod has a groove out to carry an O-ring seal which slides in a water-cooled housing against a lubricated surface. The rod carrying the crucible is driven by a velodyne motor through a gearbox and a precision lead screw to provide lowering rates in the range 0.01 to 1.00 mm/min. Typical lowering rates for rare earth fluoride systems were 0.2 mm/min.

Radio-frequency power at 300 kHz was provided by a generator with a capability of 25 kW of continuous power. An r.f. coil of 6 turns was used; this was made of copper tube and water-cooled.

The crucibles were made by machining graphite rods (Ultra-Carbon UF 4S grade). They were cylindrical (6 mm bore and overall length 180 mm) with a conical bottom and a capillary (~ 1 mm bore) seeding tip.

The usual procedure was to fill the crucible with powder at the required composition.

(46) Stockbarger, D.C., 1936, Rev. Sci. Inst., 7, 133.

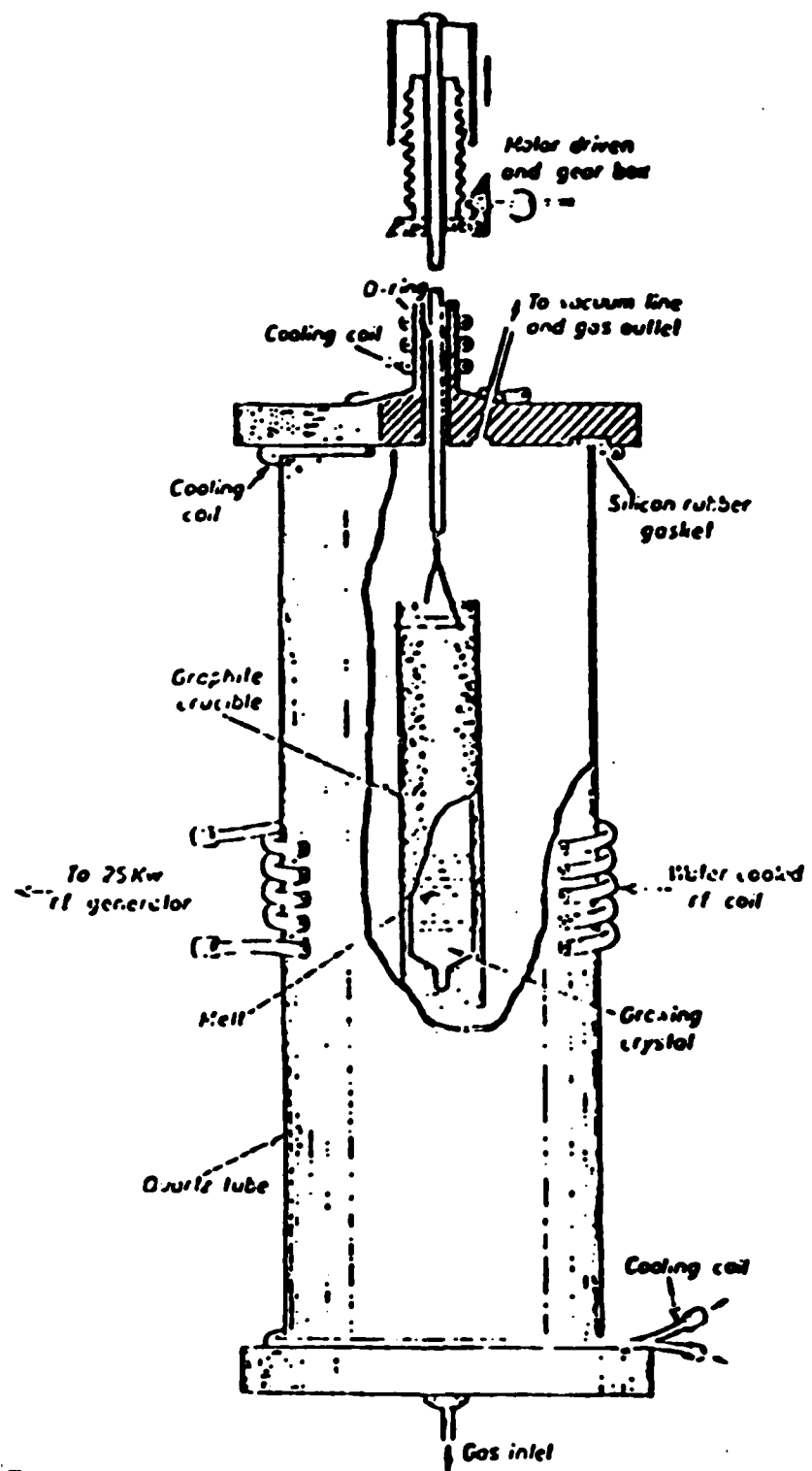


FIGURE 3

CRYSTAL GROWING APPARATUS
(NOT TO SCALE)

The crucible was then attached to the drive rod and positioned so that its base was in the centre of the r.f. coil. The work chamber was then evacuated and flushed several times with argon (B.O.C. Ltd.) and finally left in a slow stream of argon. The r.f. was turned on and the power increased until the powder had melted. This was judged by readings from an optical pyrometer. The drive motor was turned on and the crucible allowed to descend through the r.f. coil. When all the melt had been judged to have crystallized the r.f. power was reduced to zero and the sample removed from the crucible.

II.3. Conductivity measurements.

The details of the conductivity cell used in this work are shown in Figures 4,5,6. The operation of the cell is fairly obvious and only the essential details of the system and its application will be mentioned.

The major features of the cell are as follows:-

- (i) the double thermocouple system allows temperature at both crystal faces to be monitored and temperature gradients to be eliminated.
- (ii) the cell atmosphere can be an inert gas, such as N₂, or a dynamic vacuum. An ionization gauge on the top of the cell (not shown in the figures) showed that vacua better than 10⁻⁶ Torr could be maintained.
- (iii) the only materials in the hot zone of the cell are silica, platinum, and graphite, which are all relatively chemically inert.
- (iv) the temperature is controllable to ± 0.2 K over short periods and to ± 0.5 K over periods of days. This is achieved by use of a RT3/RMK2 (AEI Limited, London) proportional controller.
- (v) A.c. conductivity measurements can be made from 100 Hz to 50 kHz using a B641 Wayne-Kerr Bridge, S121 Wayne-Kerr Signal Generator, and Waveform Analyser and a Tektronix Oscilloscope. Additional measurements could be made from 500 kHz to 108 MHz with a Hewlett-Packard 4815A R.F. vector impedance meter.

The samples for conductivity measurements were cylinders, typically 10 mm long with a diameter of 4 to 6 mm. This shape was also ideal for the N.M.R. samples. Where necessary they were ground in this shape on fine emery paper and washed with Analar acetone (clearly, crystals grown in

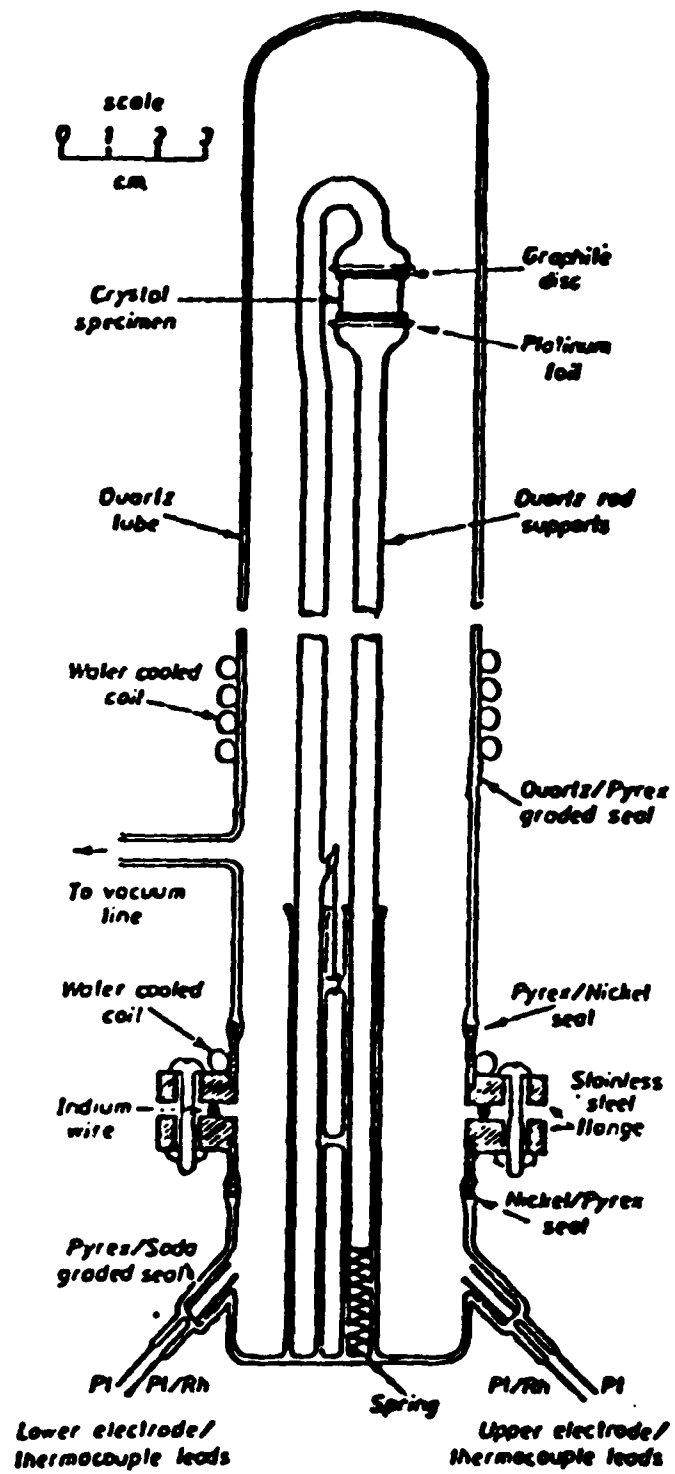


FIGURE 4

CONDUCTIVITY CELL "B"

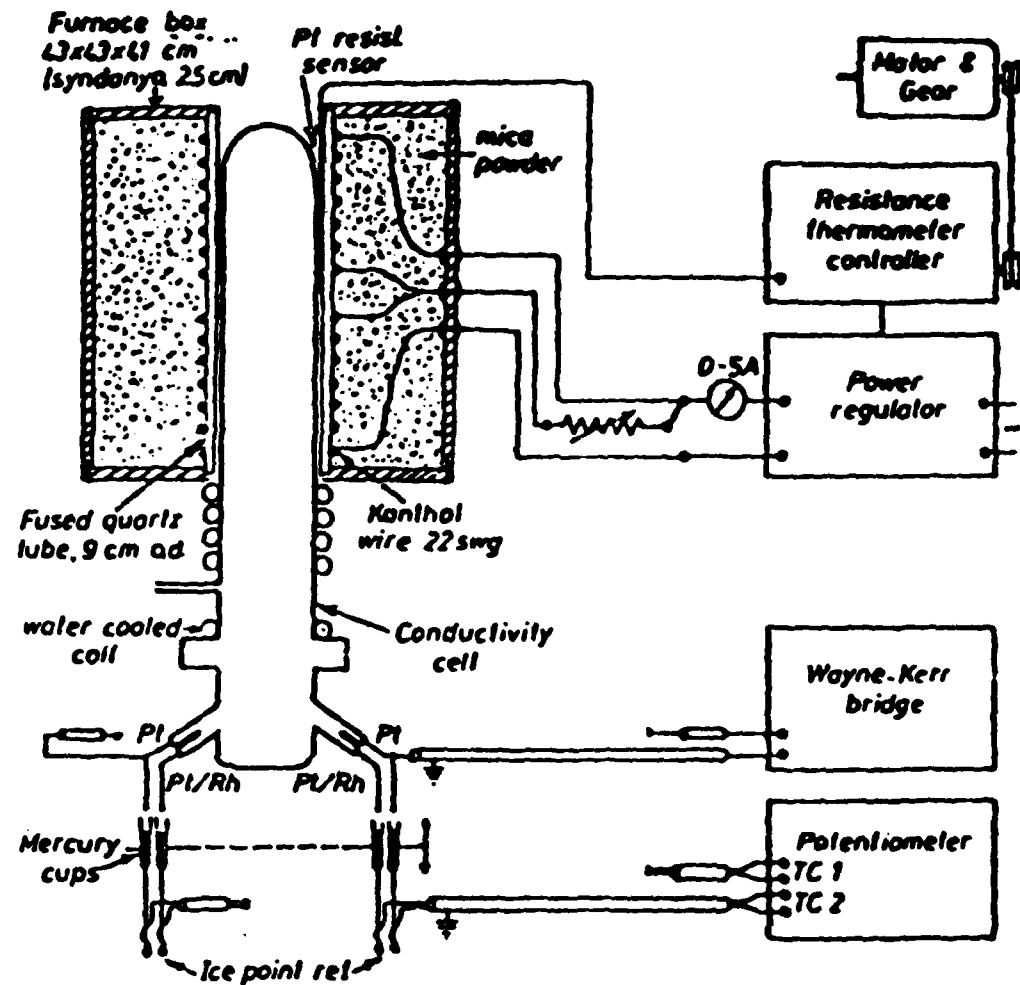
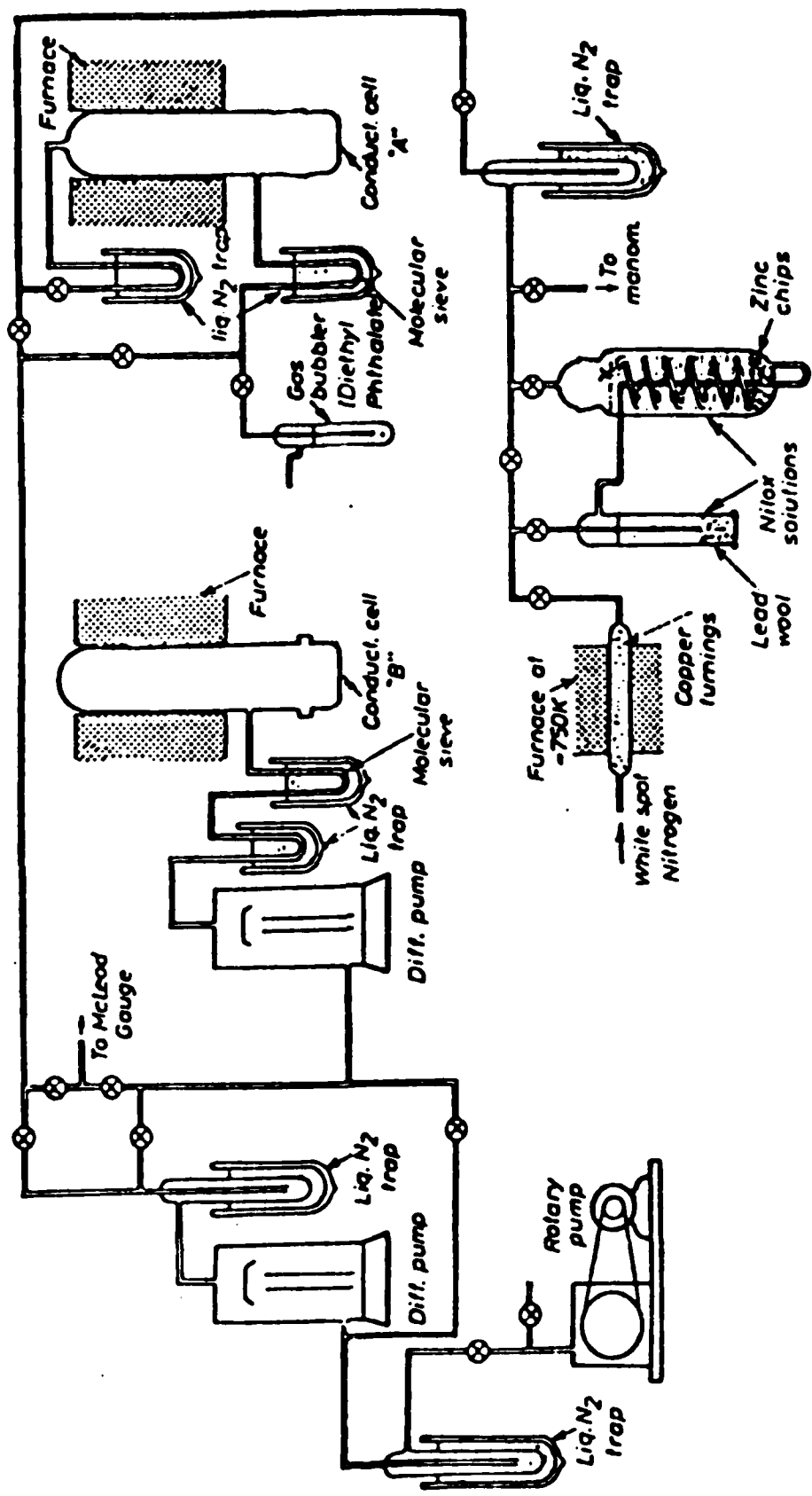


FIGURE 5

EXPERIMENTAL SET-UP FOR MEASUREMENT OF CONDUCTIVITY
AND TEMPERATURE.



VACUUM SYSTEM AND GAS PURIFIER
FOR THE CONDUCTIVITY APPARATUS.

FIGURE 6

our laboratory needed the minimum of preparation due to the design of the crucible). The two flat faces were coated with graphite by the application of several thin coats of Acheson DAG (a colloidal suspension of graphite in isopropyl alcohol). The sample was then loaded into the cell and the system pumped out for 48 hours.

All the present measurements were made with a high vacuum in the cell. Conductivity measurements were made at 5K intervals of increasing and decreasing temperature and careful checks made of the reproducibility of the results. For each data point the system was allowed to reach thermal equilibrium which usually took about 20 mins.

II.4. N.M.R. Measurements

(a) The relaxation time measurements are made using a high powered phase coherent pulsed N.M.R. spectrometer manufactured by Polaron Instruments Limited (London), operating at 10 MHz. Figure 7 shows a block diagram of this spectrometer indicating its main features. A crystal controlled oscillator generates a continuous r.f. signal which is split into two channels; each one goes to r.f. gates via delay lines. The delay lines act as phase shifters to control the phase difference between the r.f. channels and a reference signal which is fed to the receiver. The r.f. gates are opened by a group of DC pulses from the pulse programmer, thus producing r.f. pulses which, after various amplification stages, are fed to the power amplifier. The amplified r.f. pulses are then taken to the N.M.R. coil around the sample via a matching network. The nuclear induction signal which results is picked up by the receiver coil and fed to a preamplifier. The N.M.R. signal is transmitted to the receiver where it is amplified further and a phase coherent detected FID (free induction decay) produced which is displayed on a Transient recorder.

The main polarizing field H_0 is provided by a Varian variable electromagnet, which for ^{19}F resonance is set at about 2.5 kgauss for the fixed r.f. frequency of 10 MHz. The appropriate pulse sequence can be selected on the program generator which provides single pulse and multipulse groups, each pulse being controllable in length at appropriate times, and can be repeated manually or automatically at selected sampling rates. The programmer also provides trigger pulses to initiate the recording of data at appropriate times.

In this work a single coil probe configuration is used. This is preferred to a cross coil system because of its mechanical simplicity and the limited space available in the magnet gap to accommodate the

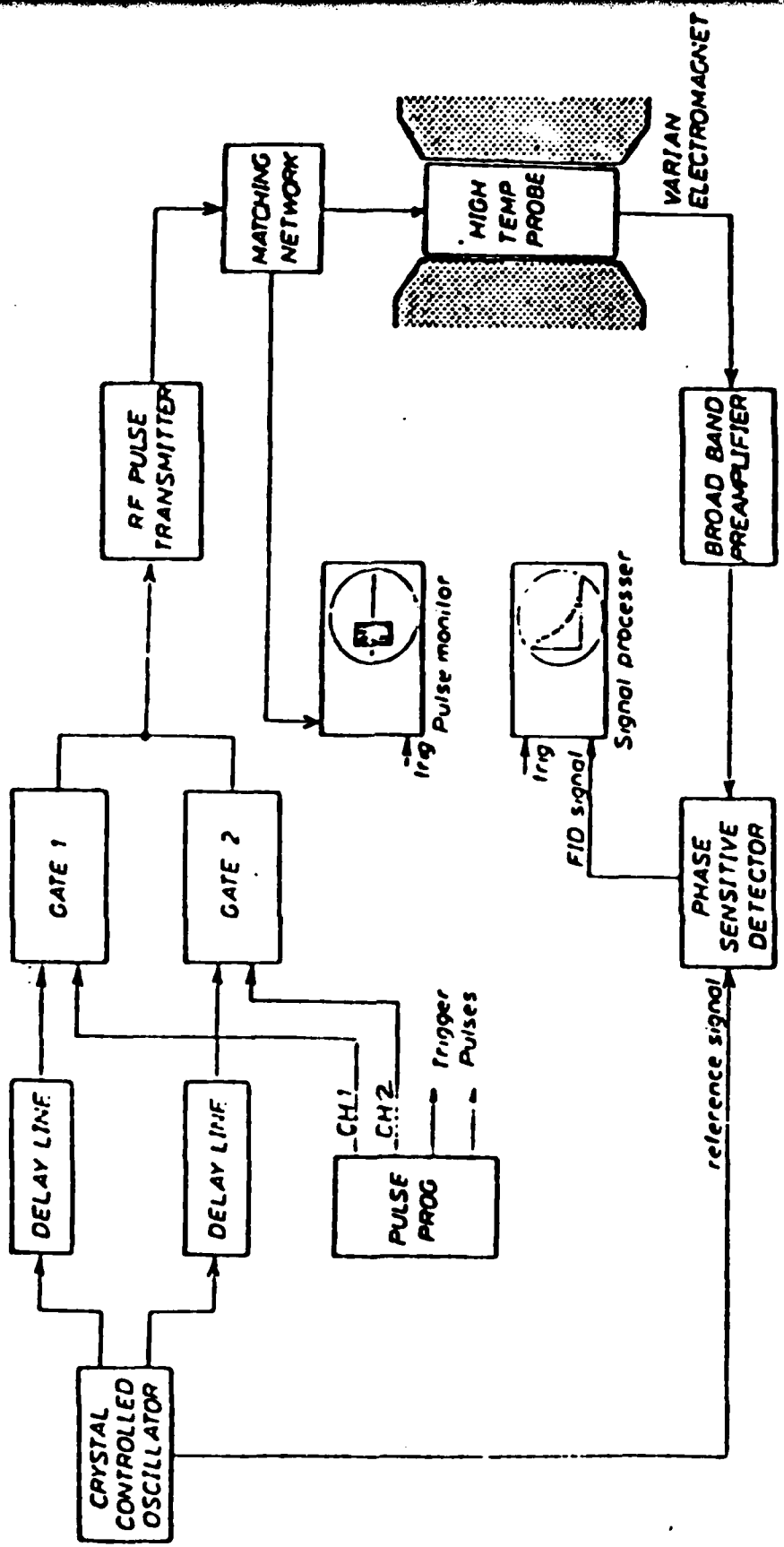


FIGURE 7 SCHEMATIC DIAGRAM OF THE PULSED NMR SPECTROMETER

thermocouple, probe, heating element, and heat insulation. The single coil has the advantage that it uses the r.f. power available from the transmitter more efficiently. In addition, it facilitates the measurements to be made for different angles between the crystal axes and H_0 , by simply rotating the whole r.f. head without altering the orthogonality required between H_1 (the pulse) and H_0 .

(b) The N.M.R. spectrometer is equipped to carry out measurements in a temperature range from room temperature to over 900°C . The heating system consists of a non-inductively wound spiral of crusilite (Morganite Ltd.) surrounding the probe. The temperature is controlled by a modified Eurotherm Controller. During operation a thermocouple with one junction at 0°C and the other inside the probe provides a voltage which is compared to the setting on the Eurotherm, and the system is maintained in dynamic equilibrium. This provides a controlled temperature with an accuracy to within a few degrees Centigrade. During pulsing and reception of signal a cutout operates on the heating system, to ensure no current is heating the spiral during a measurement.

The probe itself is a single piece of pyrophyllite designed to fit inside the heating spiral. The sample tube is cemented inside this piece of pyrophyllite, and the single coil is wound on the pyrophyllite, which acts as a former. The system as used here measures crystals with the dimensions 4 mm x 12 mm, and the coil is made of about 26 turns of gold wire. The thermocouple used is of two types; for lower temperatures a Pallador (Platinum-Palladium) is best suited, while the highest temperatures require a Rhodium Platinum thermocouple. Thermocouples can be changed easily during a single run, and provide a continuity in the temperature range.

After detection the N.M.R. signal is analyzed by direct measurement

of the visual display on a transient recorder DATALAB DL905 with incorporated CRO unit EV8000. In some instances, for example, for weak signals from powdered samples, a signal averager was fed from this recorder, and average displays obtained. Because of the small size of the samples, the size of the signal to noise ratio precluded any analysis of the exact shape of the FID.

Measurement of T_1

The spin-lattice relaxation time T_1 or F^{19} can be measured using several different techniques, depending on the magnitude of T_1 . Normally, however, only one method is used for LaF_3 . For $T_1 \leq 2$ seconds (as found with our samples) the measurements were made employing the standard two-pulse method ($90^\circ_X - \tau - 90^\circ_X$). A short r.f. pulse is applied to the sample (which is initially in thermal equilibrium and hence has its magnetisation pointing along the strong 2.5 kgauss field H_0). The time duration of this initial pulse can be finely controlled, such that it is just long enough to cause the sample magnetisation to precess rapidly into the direction perpendicular to H_0 . The pulse is typically of the order of 3-5 μsec . This is long compared with the time taken for the magnetisation to precess several times around H_0 with a Larmor frequency of 10 MHz, i.e. 0.1 μsec . After this initial pulse, the system is allowed to recover its thermal equilibrium during a time τ . As the decaying transverse magnetisation precesses around H_0 it induces a signal in the N.M.R. gold coil. The coil now acts as a receiver of signal, and the result is amplified and visually displayed. After the time τ a second 90° pulse is applied. This has the effect of producing a second FID (free induction decay) signal. Usually it is assumed that the second FID has an amplitude given by

$$M_z(\tau) = M_\infty(1 - e^{-\tau/T_1}),$$

where T_1 is the spin-lattice relaxation time. A series of measurements, for various values of τ , gives T_1 .

Measurement of T_2

The spin-spin relaxation time T_2 in LaF_3 is usually much shorter than T_1 . The methods used were dependent on the actual magnitude. For very fast FID decays, the only method available was a direct measurement of T_2^* . This may be regarded as an approximation to the 'true' T_2 if the formula $\frac{1}{T_2^*} = \frac{1}{\bar{T}_2} + \frac{1}{T_2}$ is accepted as valid. Here T_2^* is the observed decay constant of the FID (assuming a single exponential fit), \bar{T}_2 is the effects due to magnet inhomogeneity, and T_2 is the relaxation time in an ideal situation. For $T_2 \ll \bar{T}_2$, $T_2^* = T_2 + O(T_2/\bar{T}_2)$. Measurements of T_2 up to about 80-100 μsecs , necessitated the use of this method.

For longer T_2^* times the method of Carr and Purcell⁽⁴⁷⁾ was used. This is a sequence of pulses given by 90° , τ , 180° , 2τ , 180° , ... in which the 180° pulses eliminate the effects of magnet inhomogeneity. The time T_2 is obtained by measuring the magnitude of the echo signals halfway between successive 180° pulses, and fitting this to $M(2n\tau) = M(0)e^{-(2n\tau/T_2)}$.

(47) Carr, H.Y. and Purcell, E.M., 1954, Phys. Rev., 94, 630.

III. RESULTS

III.1. Sample Quality

In the first year of the project considerable time was spent in developing the crystal growing techniques.

Our initial attempts to grow pure LaF_3 crystals were unsuccessful. We used Koch-Light high purity powder but the procedures always yielded glassy, black samples. As soon as we changed to the B.D.H. zone-refined pieces or Rare Earth Products material as the starting material, good, clear single crystals were produced. A possible explanation of these results is that the Koch-Light material was produced from starting materials that had been purified by ion-exchange techniques. Thus this LaF_3 could have contained some organic materials which carbonized to very fine particles during growth and hence the black product.

Using mainly Rare Earth products materials we have grown nominally pure LaF_3 , alkaline earth fluoride doped LaF_3 , thorium (IV) fluoride doped LaF_3 . The phase change in YF_3 precluded the growth of good single crystals of this material but we have grown good crystals of NaYF_4 .

All the LaF_3 that we obtained from commercial sources were found to have fairly complex electron spin resonance, E.S.R., spectra. Obviously this suggests the presence of rare earth impurities with unpaired spins. Unfortunately, the presence of paramagnetic impurities puts severe restraints on the interpretation of the N.M.R. results^(47a). Therefore a special sample of LaF_3 powder was prepared from La_2O_3 and HF. This was relatively "clean" with a low paramagnetic impurity content.

(47a) See, for example, reference (23).

III.2. Conductivity Results

Conductivity measurements have been made on several samples of LaF_3 . The results will be described in four sub-sections.

- A. Nominally pure LaF_3
- B. Oriented LaF_3
- C. Sr^{2+} doped LaF_3
- D. Th^{4+} doped LaF_3 .

Before we go on to those sub-sections a few general remarks are necessary.

The conductivity plots - $\log \sigma T$ versus $1000K/T$ - for four crystals are shown in Figure 8. In this figure the curves have been designated as follows:-

1. B.D.H. high purity crystal. This is the purest crystal that we have been able to obtain.
2. A crystal grown from one batch of Rare Earth Products material.
3. A crystal grown from the same material as 2 plus 1000 p.p.m. SrF_2 (Harshaw crystal pieces).
4. A crystal grown from the same material as 2 plus 1000 p.p.m. ThF_4 (B.D.H. powder).

In all the crystals that we examined the conductivity showed a dependence on frequency at low frequencies. This was mentioned in our previous reports but we now have more data on which to rationalize the phenomenon. At all temperatures the conductivity at 1592 Hz was lower than that measured at higher frequencies. The exact nature of the frequency dependence depended on the geometric factor, G_F , of the crystal (length \div cross-sectional area) and the thermal history.

For crystals with $G_F > 4 \text{ cm}^{-1}$ the "as-loaded" crystal showed a conductivity at 1592 Hz about 5 to 10% lower than that at higher frequencies. On heating the crystal this discrepancy increased to about 30% at 1000K. For crystals with $G_F < 2 \text{ cm}^{-1}$ the "as-loaded"

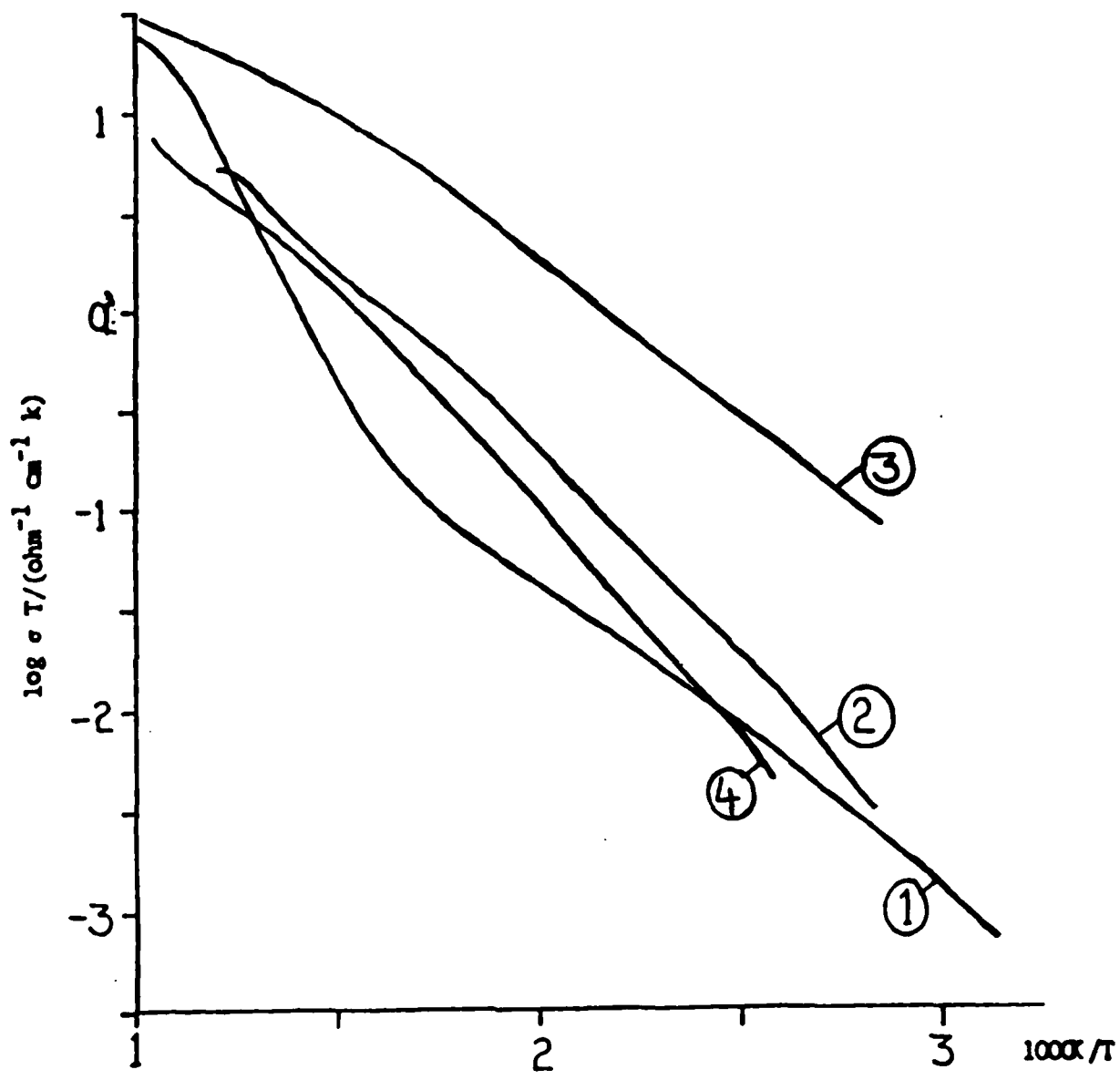


FIGURE 8 THE A.C. CONDUCTIVITY OF SEVERAL LaF_3 CRYSTALS

crystal often exhibited a conductivity at 1592 Hz about a factor of 10 lower than that at higher frequencies. On annealing at 650 K and cooling at 1K per minute to room temperature this large discrepancy was reduced so that the conductivity at 1592 Hz was only a few per cent below that at higher frequencies. This annealing did not affect the high frequency conductivity. On subsequent heating these crystals behaved in a similar manner to those with a larger G_F . For all crystals the conductivity at frequencies ≥ 10 kHz were frequency independent. It is only the frequency independent results that are shown in Figure 8 and for other crystals mentioned in this report.

The conductivity of all crystals was reproducible on thermal cycling below 1000K. If this temperature was exceeded the conductivity at lower temperatures was generally increased. This was presumably due to a high temperature reaction of the crystals with traces of O_2 or H_2O in the cell atmosphere leading to O^{2-} doping.

For most crystals the conductivity plots at the highest temperatures exhibited a region of decreasing slope. A related phenomenon was that the more impure crystals tended to show no intrinsic behaviour. This is seen for crystal 2 in Figure 8, the plot cuts across the intrinsic region of the purer crystal 1.

The frequency dependence and the region of low slope in the conductivity plots at the highest temperatures probably have a common origin. They could both be explained quantitatively in part by the presence of a temperature independent resistance, of about 100 to 1000 ohms, in series with the crystals. By analogy with our previous work on BaF_2 ⁽⁴⁸⁾ and the capacitance measurements on LaF_3 ⁽⁴⁹⁾ the origin of this surface

(48) Carr, V.M., Chadwick, A.V. and Figueroa, D.R., 1976,
J. Physique 37 C7 - 337.

(49) Solomon, R., Sher, A. and Muller, M.W., 1966, J.Appl. Phys.,
37, 247.

resistance could be a surface layer of oxide formed by a reaction with O_2 or H_2O during the cutting and preparing the samples or during the conductivity measurements. However, there are two curious features that have to be explained. The first of these is the reduction of the frequency dependence in crystals with $G_F < 2 \text{ cm}^{-1}$ at 650 K. It could be argued that this is due to the oxide layer diffusing into the bulk. If this were the case it seems odd that the frequency dependence should not disappear completely. In our work on $\text{BaF}_2^{(48)}$ we found that at high temperatures the low frequency was not reproducible and decreased with time, due presumably to a build up of a surface oxide layer with time. This is not the case with LaF_3 , the conductivity although frequency dependent, was not time dependent at high temperatures. To explain these effects one has to invoke a quasi-static oxide layer where the production rate and diffusion rate into the crystal were virtually exactly balanced. This seems to be unlikely.

III.2 A. Nominally pure LaF₃

A number of nominally pure crystals have been investigated in the course of this work and some of the data have been reported in our previous reports. The results of two crystals merit attention as they bring out the major features of nominally pure crystals. These are the high purity B.D.H. crystal which was designated crystal 1 in Figure 8. A high density of data points was taken for this crystal and they were used to test the computer analysis developed in Section I.4. The data for this crystal are shown separately in Figure 9. Crystal 5 was a crystal grown by Optovac Limited and kindly donated to us by Professor J.J. Fontanella (U.S. Naval Academy). This crystal was of known orientation, measurements were taken // to the c-axis, and the results are shown in Figure 10.

A comparison of Figures 9 and 10 shows that crystal 5 is heavily doped. It shows no sign of intrinsic behaviour. In fact, the conductivity of this crystal is similar to that for the deliberately Sr²⁺ doped crystal c.f. Figures 10 and 8.

The high temperature region of crystal 1, the region of decreasing slope, was regarded as anomalous and was not used in the computer analysis. The model and equations developed in Section I.4 were used without further modification and the results shown in Table 1 were obtained. The fit to this model is reasonable. In the alkali halides that have been computer analysed the standard deviations for the best fits are around 1 to 3×10^{-3} . Thus the present value of 7.71×10^{-3} is at least comparable with those results and is encouraging. It is very difficult to estimate the errors on the parameters from this type of fitting, however, the enthalpies should be good to ± 0.1 eV and the entropies to $\pm 1k$. As would be expected the enthalpies are not very different from the Arrhenius energies obtained from the slopes of linear regions of the conductivity plot.

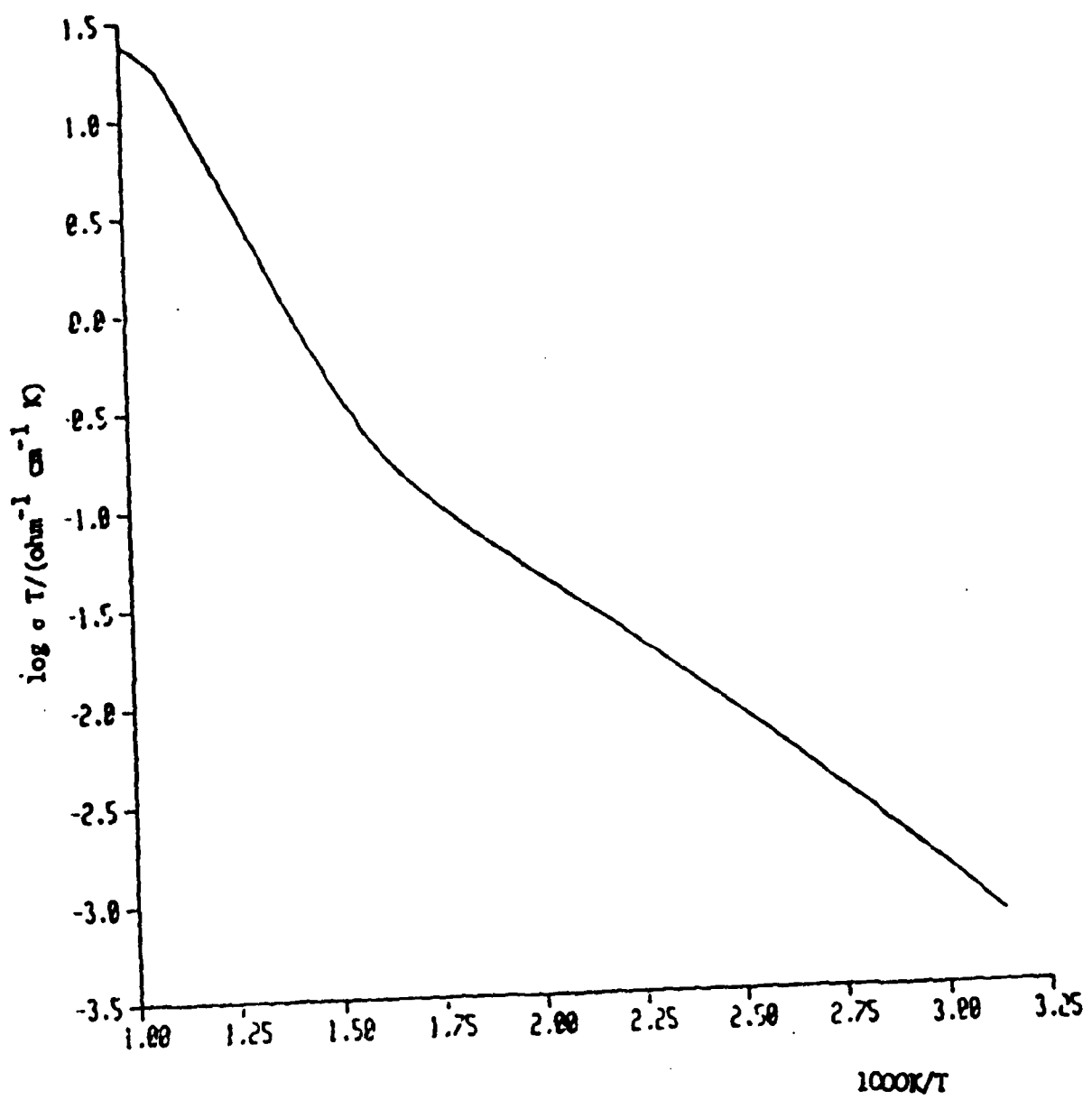
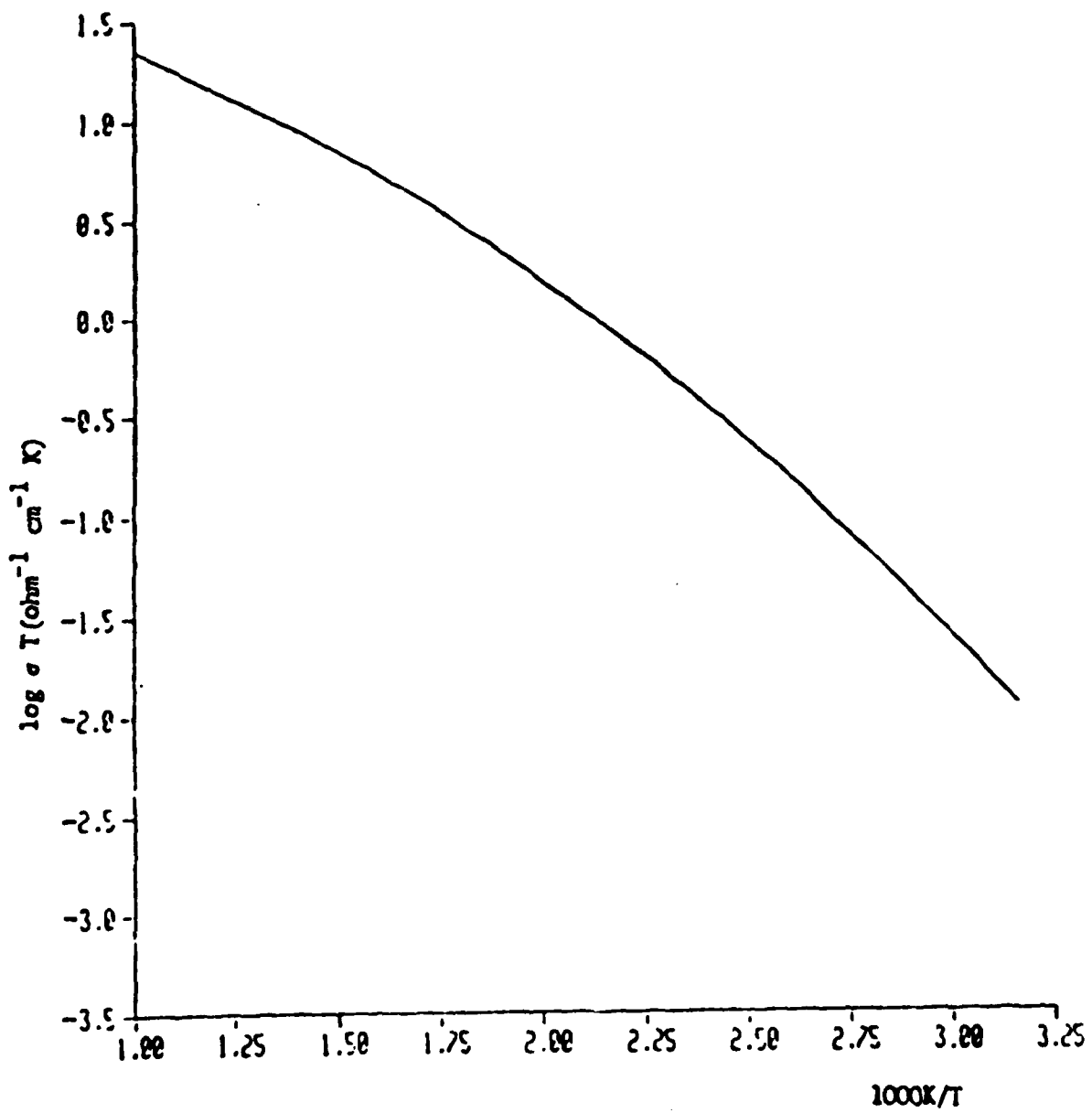


FIGURE 9 THE A.C. CONDUCTIVITY OF PURE LaF_3 CRYSTAL 1.



• FIGURE 10 THE A.C. CONDUCTIVITY OF AN OPTOVAC SAMPLE
OF LaF_3 CRYSTAL 5.

TABLE 1

Computer fitting of pure LaF₃, crystal 1

Parameter	Computed Value	Arrhenius Parameters for LaF ₃
h_s/eV	2.12	2.24
s_s/k	0.002	
h_{mP}/eV	0.28	0.24 - 0.28
s_{mP}/k	1.65	
h_{mLn}/eV	0.58	
s_{mLn}/k	0.02	
h_a/eV	0.37	0.20 - 0.48
s_a/k	6.14	
c_M^T	191×10^{-6}	
No of data points	70	
Standard deviation	7.71×10^{-3}	

* Evaluated from linear regions of the conductivity plot.

Further discussion of the fitting will be left until Section IV, however, it is worth mentioning that since M^{2+} , M^+ or O^{2-} impurities would all create F^- vacancies in LaF_3 the model will not discriminate which of these impurities is present in crystal 1.

III.2 B. Oriented LaF₃

The crystals which we have grown are in the form of cylinders and are not ideally suited for studies of the orientation dependence of the conduction. For these experiments we obtained three 6 mm cubes all cut with the same relative orientation off a large boule from B.D.H. Limited. An X-ray determination of the crystal orientation of one of these cubes was performed by Dr. J.D. Wright (University of Kent). This showed that one face was parallel to the c-axis, to within about 5°, and another was parallel to either the a or b-axis. The X-ray analysis could not distinguish between the a and b axes.

For a second cube the conductivity was carefully measured across each pair of faces as a function of temperature. The results are shown in Figure 11. The conductivities along the two directions \perp to the c-axis were the same, within 5% and only one of them is shown in the figure. The conductivity \parallel to the c-axis is higher than \perp to the c-axis. The anisotropy was 2.0 at room temperature and decreased to 1.4 at 650 K. These measurements were checked several times. Unfortunately the crystals were not highly pure and exhibited only extrinsic behaviour.

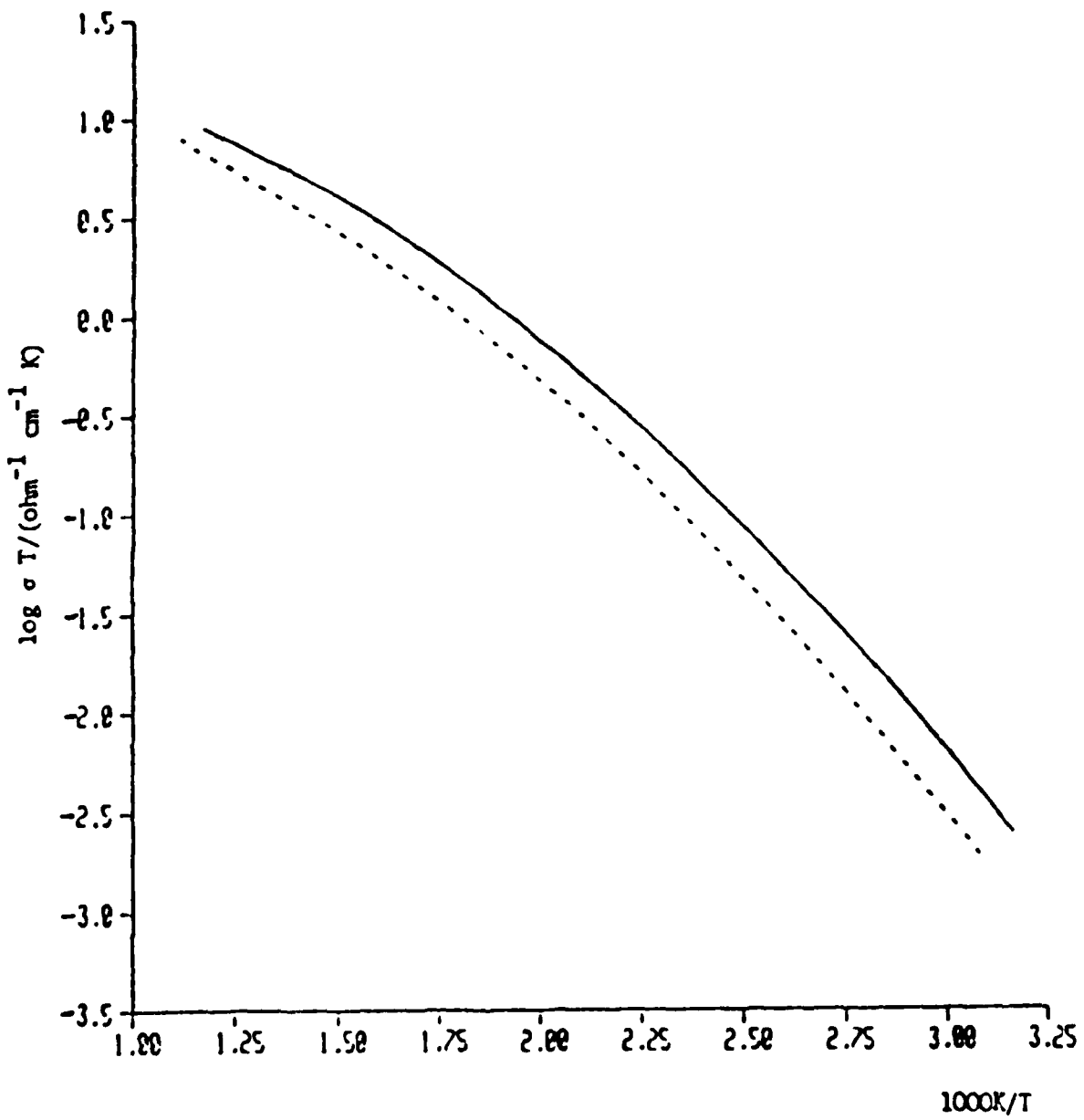


FIGURE 11 THE A.C. CONDUCTIVITY OF ORIENTED LaF_3 .

— // c-axis
- - - ⊥ c-axis

III. 2 C. Sr^{2+} doped LaF_3

Crystal 3 was doped with 1000 p.p.m. SrF_2 and the conductivity plot is shown in Figures 8 and 12.

As might have been expected the conductivity of this crystal has been considerably increased, to such an extent that there is no extrinsic behaviour in the region studied. The curve is parallel to that of the undoped starting material, crystal 2.

In the past year we have extended the study of Sr^{2+} doped LaF_3 crystals to heavily doped systems. In Figure 12 we show the results for crystals nominally doped with 5 and 10% Sr^{2+} . These concentrations are those of the initial mix used in crystal growth and are only indicative of the level of doping. They will not be exact due to the effect of zone-refining during crystal growth.

The first point to note is the very high conductivity of these systems. Secondly, the conductivity is increasing with dopant concentration. It does not appear to be linear, however, without more exact information on the dopant concentration this point cannot be tested. It should be noted that the 10% doped crystal had to be regrown several times before a good, clear sample was obtained. This suggests that 10% doping is approaching the solubility limit of Sr^{2+} in LaF_3 .

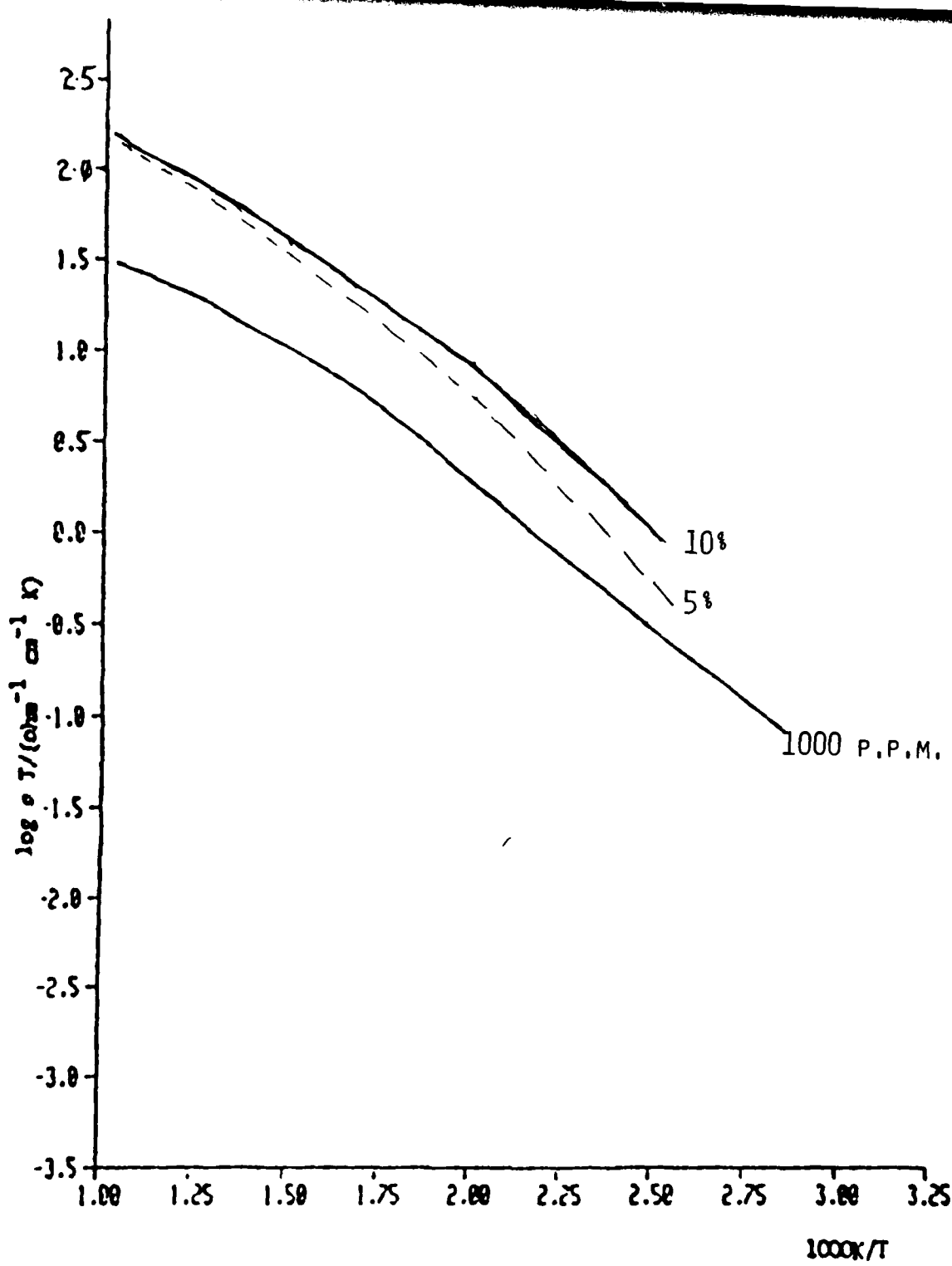


FIGURE 12 THE A.C. CONDUCTIVITY OF LaF_3 DOPED WITH SRF_2

III.2 D. Th⁴⁺ doped LaF₃

Crystal 4 was doped with 1000 p.p.m. ThF₄ and the conductivity plot is shown in Figure 8 and 13.

The conductivity has been reduced from that of the undoped starting material, crystal 2. However the effect is very slight and the curve is still roughly parallel to crystal 2. This could be due to there being insufficient Th⁴⁺ present in the sample to compensate for the natural impurities in the starting material.

In the last year studies were also made of a crystal nominally doped with 1% ThF₄. The conductivity of this crystal is even lower than that doped with 1000 p.p.m. ThF₄. This suggests that very little Th⁴⁺ is actually dissolving in these crystals and that only in the higher doped crystal is the effect of excess Th⁴⁺ in the lattice is being observed. In the higher doped crystal the activation energy is higher than in the Sr²⁺ doped crystals and is approximately 0.5 eV. On the basis of a Shottky model for the dominant disorder in LaF₃ this means that the migration enthalpy of the La³⁺ vacancy is 0.5 eV.

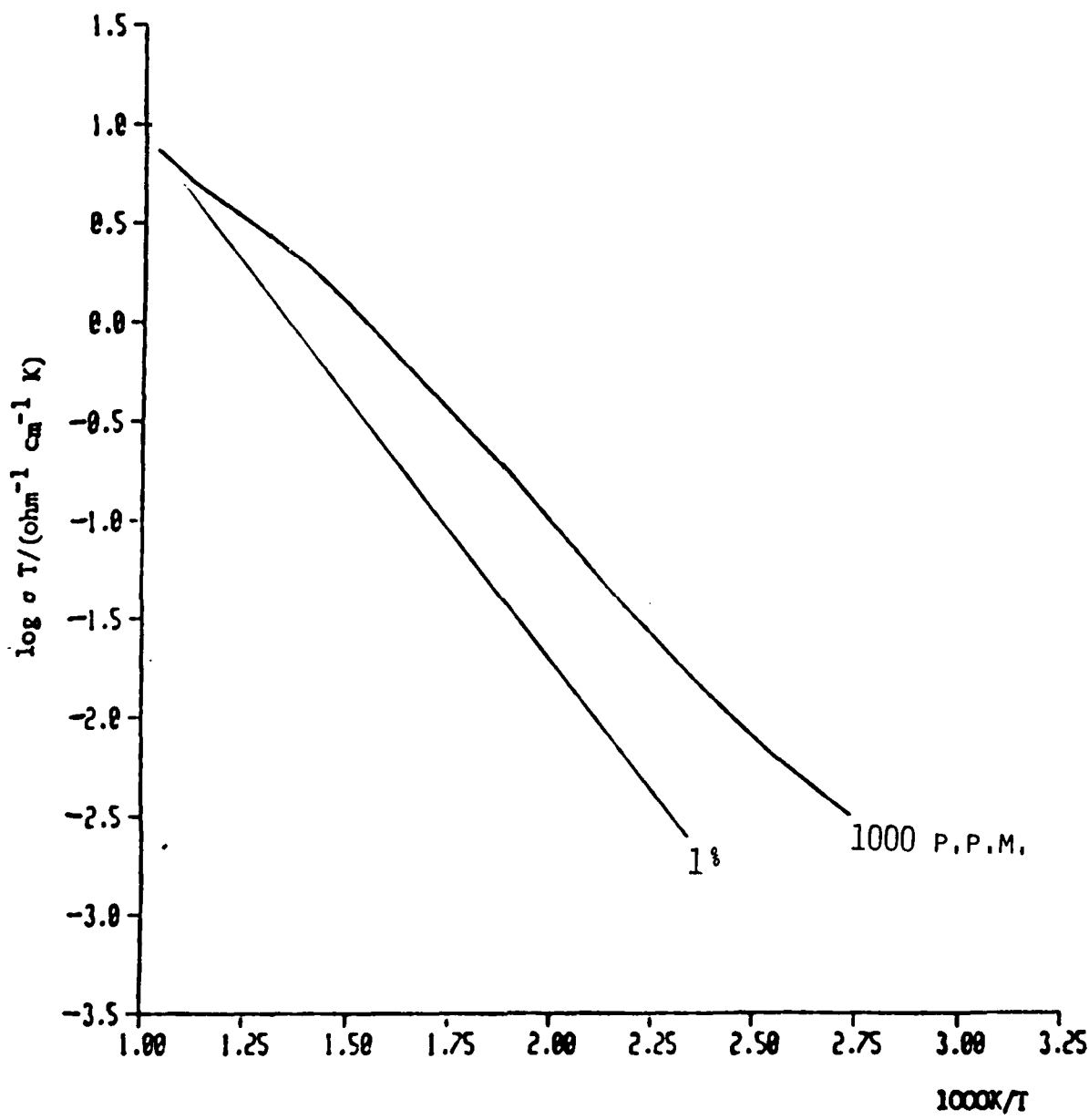


FIGURE 13 THE A.C. CONDUCTIVITY OF LaF_3 DOPED WITH ThF_4

III.3. N.M.R. Results.

III.3 A. YF₃

Since it is not possible to grow single crystals of YF₃ a useful comparative study of conductivity and N.M.R. in this material is not possible. However, a brief study was made of the N.M.R. of a powdered sample obtained from Koch-Light Ltd.

As the sample was a powder the signal was small and only measurements of T₁ were taken. The results are shown in Figure 14. The powder was doped with 0.5% BaF₂ and an unsuccessful attempt was made to grow a crystal. T₁ was measured for the doped powder and the results are also shown in Figure 14. The values of T₁ for both samples suggest that the relaxation was dominated by paramagnetic impurities up to about 500K. Above 500K the effects of motional narrowing are evident. The Arrhenius energy of the motionally narrowed region is 0.39 eV.

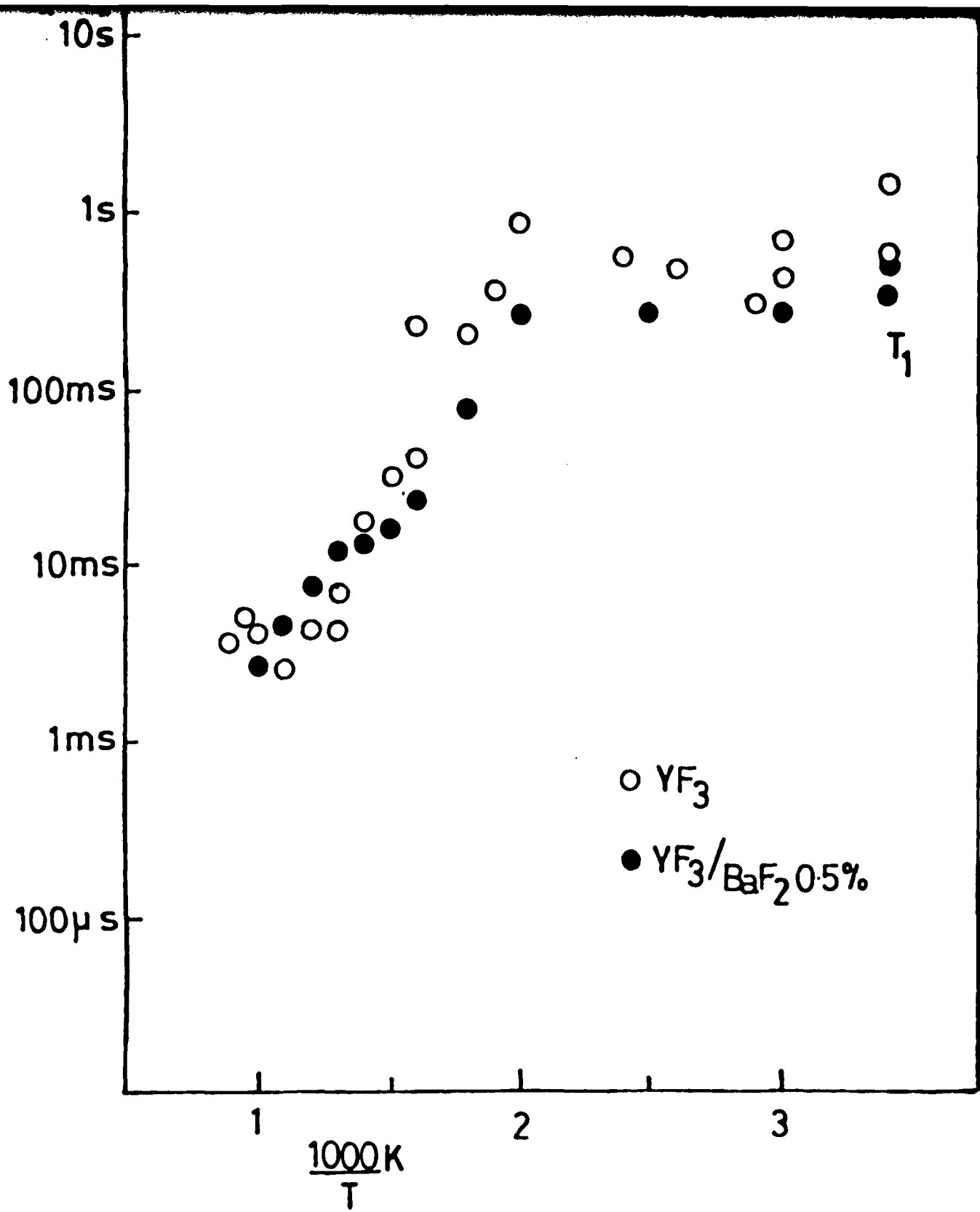


FIGURE 14 SPIN-LATTICE RELAXATION TIMES FOR UNDOPED AND DOPED YF_3 .

III.3 B. LaF₃

In all the N.M.R. measurements it was found that the relaxation times were reproducible on cycling below 1000K. This was expected as oxidation effects would be limited to the surface layers of the sample and would not affect the N.M.R. The N.M.R. signal is an "average" for the whole sample.

In the initial stages of the project measurements were taken on commercial powdered samples. These were mainly used to set up the spectrometer and the bulk of the work was concentrated on single crystals.

T_1 , T_2 and $T_{1\rho}$ measurements were taken over a wide range of temperatures for the crystals 6 (a piece of B.D.H. zone-refined material) and 7 (a crystal grown from B.D.H. zone-refined material). The conductivities of both these nominally pure crystals were thoroughly studied and the results are shown in Figures 15 and 16. The orientation of crystal 6 was unknown. Crystal 7 was cut from the boule so that its long axis was the crystal growth axis. This crystal was set up in the spectrometer so that it could be rotated about this axis and the strong main field of 2.5 kgauss was perpendicular to this axis. It seemed likely that the growth axis was the c-axis of the crystal. If this hypothesis is correct then the angular dependence of T_2 should display maxima separated by 60 and 120°, corresponding to the a and b crystal axes, when rotated in the main field. This was found to be the case, as can be seen in the T_2 results at 400K which are shown in Figure 17. The orientation corresponding to position A on this graph was retained in all the subsequent experiments.

The results for crystals 6 and 7 are shown in Figures 15 and 16 and Table 2 lists the Arrhenius energies found from the graphs. These

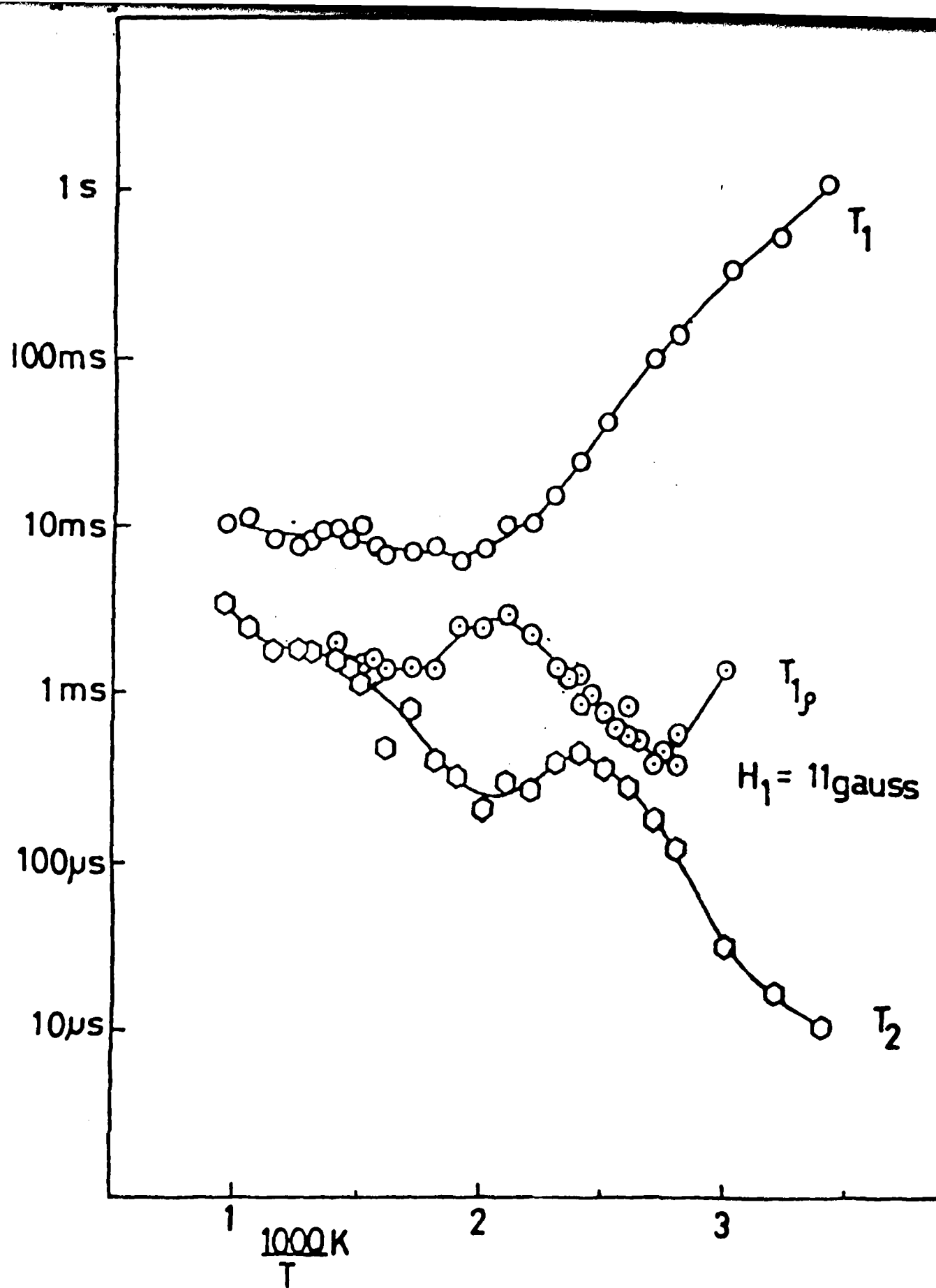


FIGURE 15 T_1 , $T_{1\rho}$, T_2 , DATA FOR CRYSTAL 6, FOR $H_1 = 11$ GAUSS

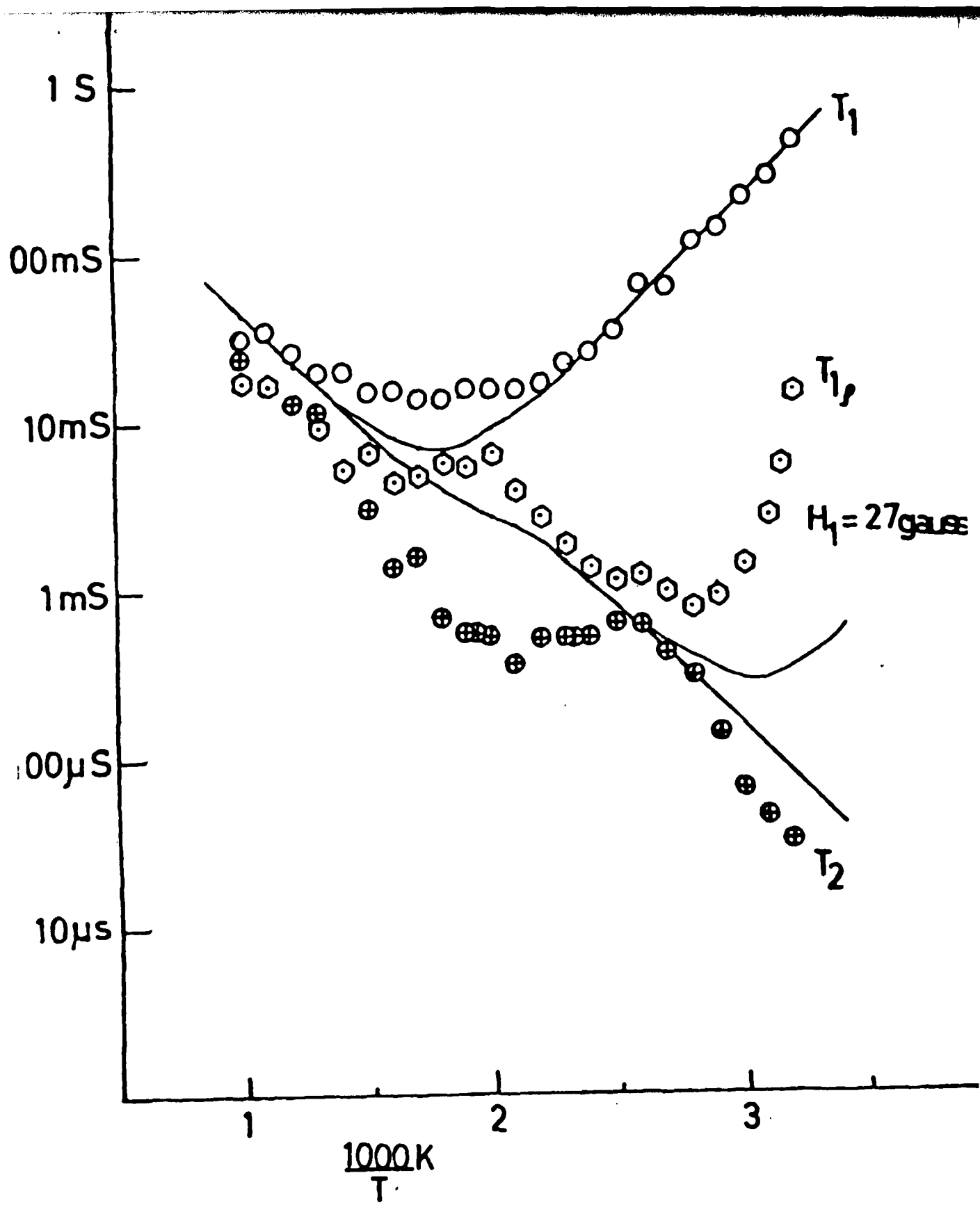


FIGURE 7 T_1 , $T_{1\rho}$, T_2 , DATA FOR CRYSTAL 7, FOR $H_1 = 27$ GAUSS.

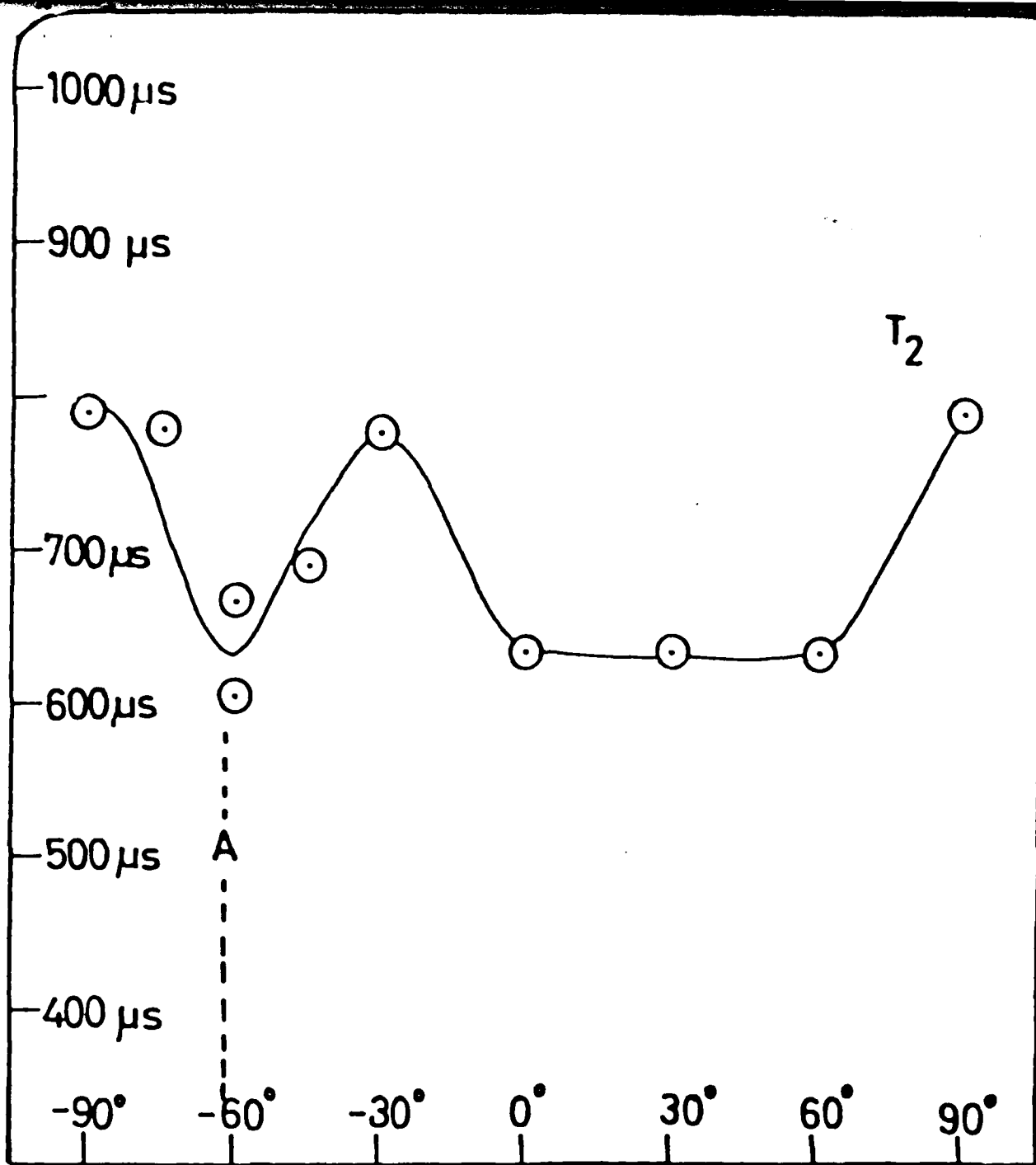


FIGURE 17 T_2 FOR CRYSTAL 7 VERSUS ORIENTATION ABOUT
 H_0 AT 400K

TABLE 2

	Crystal 6	Crystal 7
T_1 low temperature	0.35 eV	0.30 eV
T_1 high temperature	0.043 eV	0.16 eV
T_2 low temperature	0.43 eV	0.55 eV
T_2 high temperature	0.16 eV	0.39 eV
$T_{1\rho}$ low temperature	0.44 eV	0.95 eV
$T_{1\rho}$ medium temperature	0.30 eV	0.32 eV

results were the first complete T_1 , T_2 and T_{10} data that had been measured for the same LaF_3 crystal.

In Figure 18 the results for crystal 7 are re-plotted and the solid lines are the fits to the theory outlined in Section I.4. The details of this fitting have been published⁽⁵⁰⁾ and only a brief description is presented here. In the Goldman-Shen model⁽²⁹⁾ sub-lattice A is the one on which the fluoride ions move relatively fast compared to those on sub-lattice B. At low temperatures, i.e. near room temperature, B fluoride ions are regarded as essentially static. Hence in this temperature regime only $\tau_{A \rightarrow A}$ is significant. At higher temperatures the local maximum is due to the exchange frequency, $\tau_{A \leftrightarrow B}$, becoming increasingly important. In the vicinity of the maximum $\tau_{A \leftrightarrow B}$ can be found if $\tau_{A \rightarrow A}$ is already known. Finally at high temperatures a non-linear least squares fit can be made to find $\tau_{B \rightarrow B}$ if $\tau_{A \rightarrow A}$ and $\tau_{A \leftrightarrow B}$ are known. Hence all three jump times can be found from the T_2 curve alone leaving the T_1 and T_{10} curves as predictions. The jump time dependence with temperature for the three types of jump are shown in Figure 19 and the Arrhenius parameters are listed in Table 3. It is interesting to note that $\tau_{A \leftrightarrow B}$, given as "EXCHANGE" is very much smaller than $\tau_{A \rightarrow A}$ or $\tau_{B \rightarrow B}$ but its effect is large on T_2 and T_{10} and is responsible for the maxima in both cases. From Figure 18 it is clear that the theory successfully predicts the position of the T_1 minimum and the features of the T_{10} data. The quantitative discrepancies are believed to be due to the approximations in the theory.

The presence of paramagnetic impurities in the commercial LaF_3 samples puts severe constraints on the analysis of the N.M.R. date. It

(50) Jaroszkiewicz, G. and Strange, J.H., 1979, Proceedings of the Third Europhysical Conference on Lattice Defects in Ionic Crystals, September, Canterbury, U.K. To be published in J. de Physique.

was hoped that these would be overcome in the powder sample of LaF_3 produced from La_2O_3 and HF. As we have mentioned the E.S.R. spectrum of this sample indicated a low concentration of paramagnetic impurity. However, the room temperature T_1 for this powder was very short, ~ few ms. This was disappointing since a sample with a low paramagnetic impurity content would have a long T_1 , the order of seconds. The short T_1 may be due to the powder showing enhanced diffusion due to other dopants, such as O^{2-} or aliovalent cations.

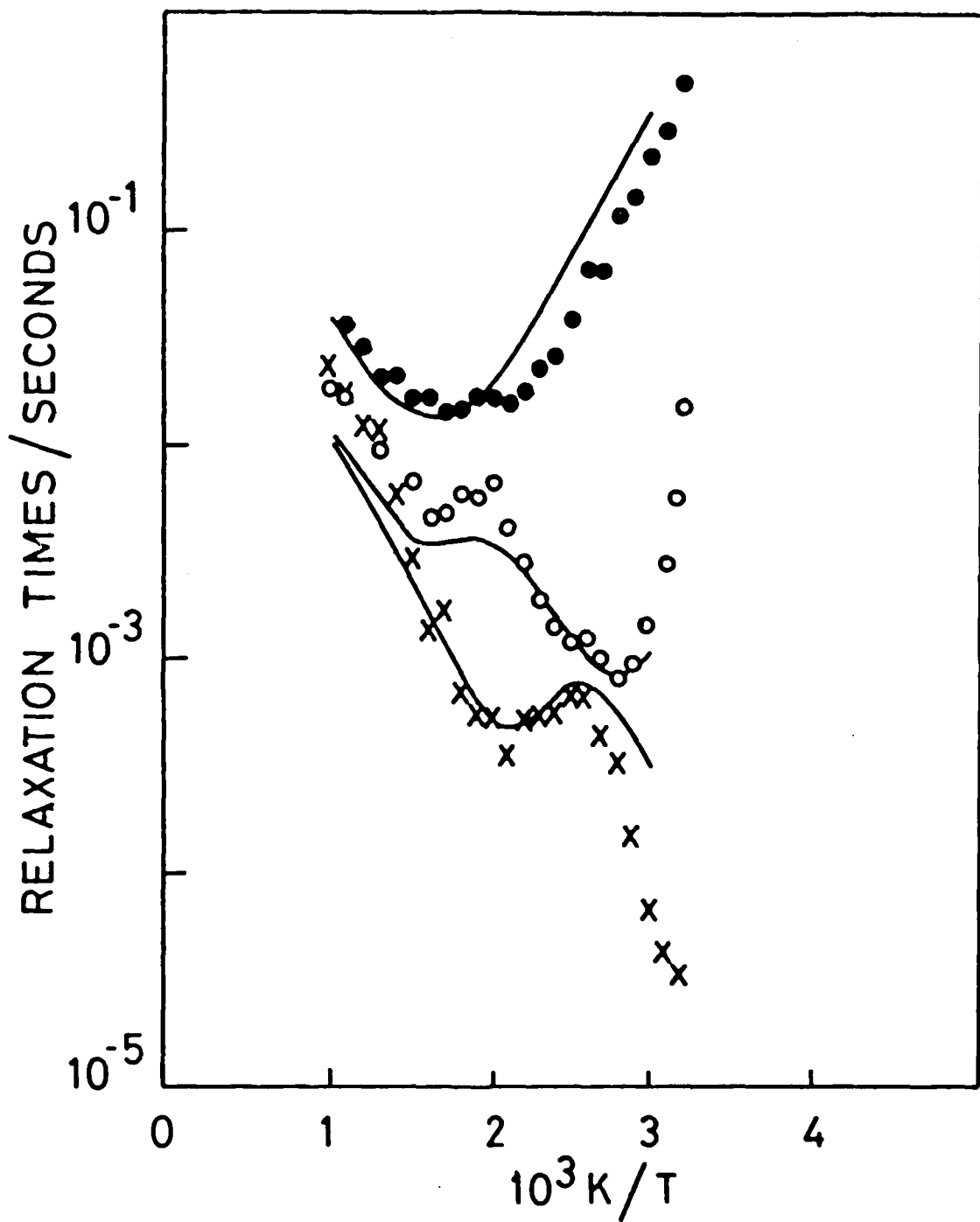


FIGURE 18

^{19}F N.M.R. RELAXATION TIMES IN LaF_3 AS A FUNCTION OF
TEMPERATURE: • • • T_1 ; ○ ○ ○ $T_{1\rho}$; × × × T_2

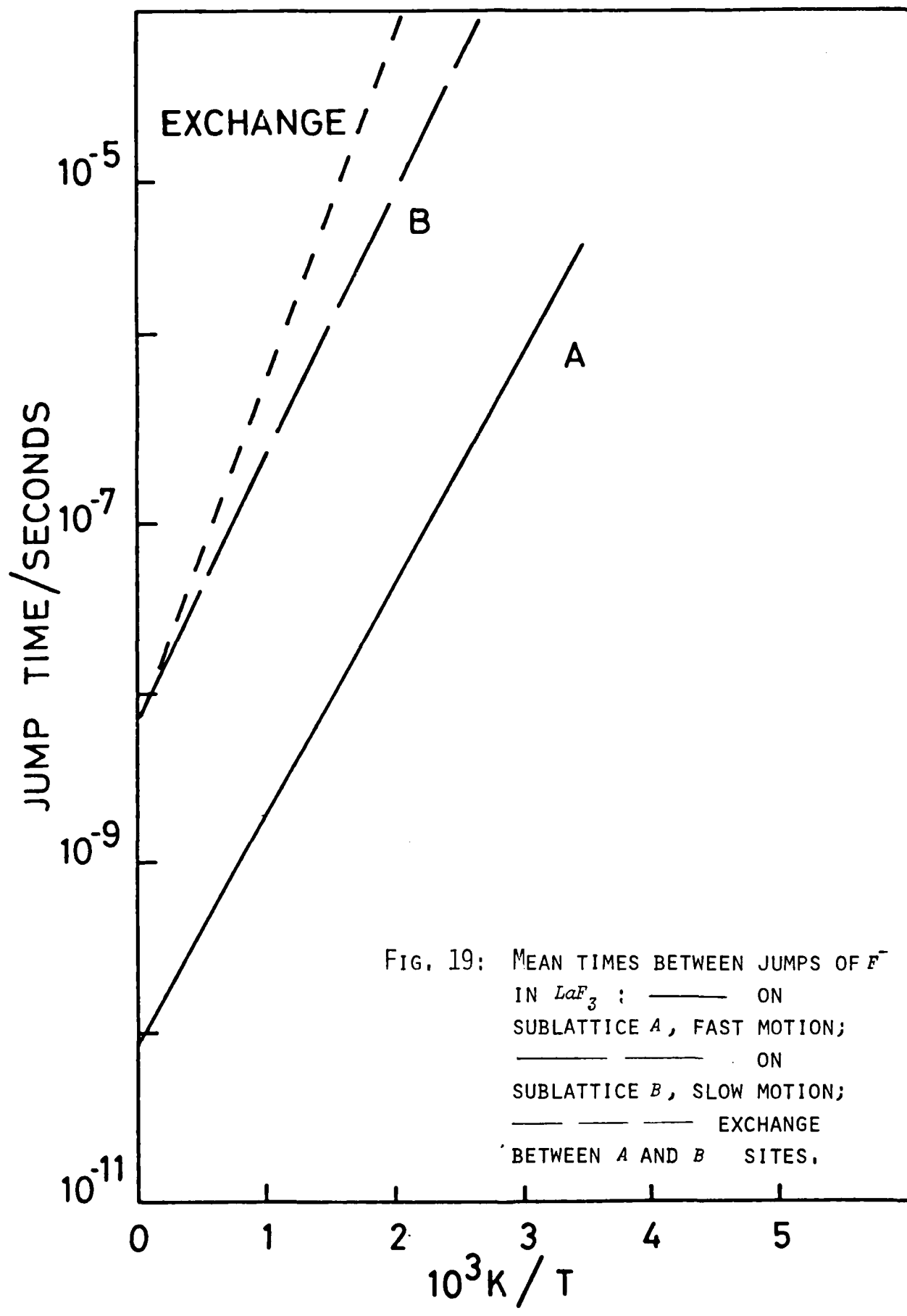


TABLE 3

	ACTIVATION ENERGY/(eV)	$v_o/(Hz)$
A(FAST) SUBLATTICE	.27	$1.2 \cdot 10^{10}$
B(SLOW) SUBLATTICE	.3	$1.3 \cdot 10^8$
EXCHANGE	.4	$1.5 \cdot 10^8$

IV. DISCUSSION

IV.1. Comparison of the present results with other transport data for LaF₃

IV.1 A. Conductivity data

The published conductivity data for LaF₃ includes the work of Sher et al⁽²⁶⁾, Fielder⁽²⁷⁾, Nagle and O'Keeffe⁽²⁸⁾, Solomon et al⁽⁴⁹⁾, Lilly et al⁽⁵¹⁾, Tiller et al⁽⁵²⁾, Schoonman et al⁽⁵³⁾ and Murin et al⁽⁵⁴⁾. Many of these data cannot be simply compared with the present results. Some of the studies have not employed single crystal samples and/or the temperature ranges employed do not overlap with the present work and/or the nature and concentration of impurity was unknown. The simplest method of making a comparison is to consider first nominally pure LaF₃ and then the doped material.

(i) *Nominally pure LaF₃*

In the last section we showed that the study of a wide frequency and the use of crystals with a large geometric factor were vital if the "true" conductivity was to be obtained. Obviously, the first comparison that we would like to make would be with other data that could verify that we had indeed measured the true conductivity. This requires the comparison of the intrinsic conductivity regions.

The earliest study of a single crystal was reported by Sher et al⁽²⁶⁾. The measurements used a d.c. technique and the results are curious. At low

(51) Lilly, A.C., LaRoy, B.C., Tiller, C.O. and Whiting, B., 1973, J. Electrochem. Soc., 120, 1673.

(52) Tiller, C.O., Lilly A.C. and LaRoy, B.C., 1973, Phys. Rev. B, 8, 4787.

(53) Schoonman, J., Oversluizen, G. and Wapenaar, K.E.D., 1980, (pre-print of paper submitted for publication).

(54) Murin, J. et al, 1980, Sov. J. Appl. Chem., 53, 1474 (in Russian).

temperatures, < 350K, the conductivity plot had an activation energy of 0.46 eV which decreased to only 0.084 eV, c.f. present results in Table 4. We can only conclude that the high temperature results are certainly erroneous. This is probably due to the fact that a.c. measurements were not employed and that their sample had an extremely low geometric factor (100 mm^2 cross-sectional area x 0.05 mm thick). Thus in our experience electrode polarization was probably dominating the results.

Fielder⁽²⁷⁾ made an extensive conductivity study of nominally pure LaF₃ using large crystals (10 mm cubes) and a.c. frequencies up to 100kHz. The data agrees with the present results in both magnitude and activation energy, as can be seen in Table 4. This is extremely encouraging. In earlier work, Fielder measured the conductivity of CaF₂⁽⁵⁶⁾, BaF₂⁽⁵⁵⁾ and SrF₂⁽⁵⁶⁾. His data has been shown to be in excellent agreement with more recent work, both at Kent⁽⁵⁷⁾ and in other laboratories⁽⁵⁸⁾.

The data of Nagle and O'Keefe⁽²⁸⁾ for a nominally pure LaF₃ crystal are also in good general agreement with the present work. It is clear from their graph that their crystal was insufficiently pure for them to observe a true intrinsic region. Thus the intrinsic Arrhenius energy can only be given a lower limit in their work.

Lilly et al⁽⁵¹⁾ and Tiller et al⁽⁵²⁾ studied thin films of LaF₃. They did note the existence of large polarization effects. The

(55) Fielder, W.L., 1966, NASA TN D - 3346.

(56) Fielder, W.L., 1967, NASA TN D - 3816.

(57) Kirkwood, F.G., 1980, Ph.D. Thesis, University of Kent.

(58) Jacobs, P.W.M., 1980, private communication.

TABLE 4

Collected conductivity data for
nominally pure LaF₃

	<u>log σT at 833K</u>	<u>Arrhenius energies (eV)</u>		
		<u>Intrinsic</u>	<u>High T Extrinsic</u>	<u>Low T Extrinsic</u>
This work (crystal 1)	0.8	0.80 ± 0.05	0.28 ± 0.05	0.38 ± 0.05
Sher et al ⁽²⁶⁾ (crystal)	-0.1	0.084	0.46	0.46
Fielder ⁽²⁷⁾ (crystal)	0.8	0.83	0.33	0.40
*Nagle and O'Keeffe ⁽²⁸⁾ (crystal)	0.7	>0.6	~0.3	~0.4
Tiller et al ⁽⁵²⁾ (Films)	—	0.80 ± 0.1	0.07 ± 0.04	0.40 ± 0.5
Murin et al ⁽⁵⁴⁾	~0.30	0.5 ± 0.05	0.31 ± 0.03	0.43 ± 0.03
Schoonman et al ⁽⁵³⁾ (crystal)	—	—	0.27 ± 0.01	0.44 ± 0.01

* Values estimated from figures in the original paper.

temperature dependence study⁽⁵²⁾ yielded intrinsic and low temperature activation energies similar to the present work but there was a curious mid-temperature region with a very low activation energy ~0.07 eV. We can only conclude this is the result of polarization effects.

The very recent paper of Murin et al⁽⁵⁴⁾ is still being translated from the original Russian. From the graphs and tables we were able to extract the data in Table 4. From the examination of their data it would appear that the samples are not sufficiently pure for a true intrinsic region to be observed.

The work of Schoonman et al was limited to a temperature maximum of 525K therefore no intrinsic behaviour was observed. The activation energies were similar to those we observed although their interpretation was different. They also measured the conductivity anisotropy and obtained σ (\parallel c-axis) / σ (\perp c-axis) equal to ~2 at room temperature. This is the result we found.

(ii) Doped LaF_3

Nagle and O'Keeffe⁽²⁸⁾ reported the first conductivity study of doped LaF_3 . They employed a sinter of $\text{La}_{0.95} \text{Sr}_{0.05} \text{F}_{2.95}$, i.e. 5% SrF_2 doped. Their results are virtually the same as we observed for the Optovac sample (crystal 5, see Figure 10) and parallel to the data for our own 5% SrF_2 doped crystal. However their data is about an order of magnitude lower. This is probably due to their use of a sinter rather than a single crystal and the inter-grain resistance was affecting their data.

Murin et al⁽⁵⁴⁾ studied sinters of LaF₃ doped with CaF₂, BaF₂, SrF₂ and ThF₄. Their data appears to be very similar to our own but we have still to complete a detailed analysis of that work.

Schoonman et al⁽⁵³⁾ studied polycrystalline samples and pressed pellets of LaF₃ and BaF₂ mixtures. Their data shows that sinters give lower results than crystals and support our interpretation of the Nagel and O'Keeffe data. It is worth noting that the conductivity of their 5% BaF₂ doped polycrystal was very close to that of our 5% SrF₂ doped crystal at 400K. They found that the conductivity isotherm (plot of σ versus (dopant concentration)) at 250K passes through a maximum at ~5% BaF₂ doping. Our results suggest that this would not be true at higher temperatures, as do the data of Murin et al.

IV.1 B. N.M.R. data

The published N.M.R. data for LaF_3 includes the line-width data of Sher et al⁽²⁶⁾, the spin-spin relaxation time, T_2 , data of Goldman and Shen⁽²⁹⁾, the T_1 and T_2 data of Shen⁽⁵⁹⁾ and the T_1 and $T_{1\rho}$ data of Ildstad et al⁽⁶⁰⁾.

Sher et al found an activation energy from the line-width data below 375K to be 0.43 eV. In the same temperature regime the T_2 study by Goldman and Shen gave 0.30 eV and the $T_{1\rho}$ study of Ildstad et al gave 0.48 ± 0.04 eV. These data, given the expected experimental errors, are consistent with our results given for crystals 6 and 7 in Table 2. The general features of the only other high temperature study, the T_2 work by Goldman and Shen, are also consistent with our results.

In general, the model proposed by Goldman and Shen, and especially in the modified version of Jaroszkiewicz and Strange⁽⁵⁰⁾, gives a qualitative fit to the N.M.R. data.

(59) Shen, L., 1968, Phys. Rev., 172, 259.

(60) Ildstad, E., Svare, I. and Fjeldy, T.A., 1977, Phys. Stat.Sol.
(a) 43, K65.

IV.2 Comparison of the conductivity and N.M.R. data.

These comparisons have to be approached with considerable caution. The reasons are fairly obvious and have been mentioned at various points in this report, however, for clarity they are worth repeating. Firstly, the inequivalence of the F^- ions is clearly delineated in the N.M.R. but not in the conductivity. Thus the comparison should be limited to the low temperature region, $< 375K$, where the N.M.R. suggests that motion of F^- is restricted to one sub-lattice. However, in this temperature region no LaF_3 that has been studied here or elsewhere is pure and the motion is controlled by impurity. Thus the effect of impurity - F^- vacancy association could be affecting both types of measurement. Obviously, it is very unwise to try to compare N.M.R. data from one set of workers with conductivity data from another set of workers when different samples have been used. They would almost inevitably contain different impurity levels and hence have different diffusion coefficients for the F^- ion. Thus the comparisons made by Ildstad et al⁽⁶⁰⁾ of their N.M.R. data with the Sher et al⁽²⁶⁾ conductivity is not meaningful. A similar comment holds for the comparison made by Schoonman et al⁽⁵³⁾ of their conductivity with the N.M.R. data of Sher et al⁽²⁶⁾.

The treatment of the N.M.R. developed in this project⁽⁵⁰⁾ show that the activation energies for all three types of motion, fast, slow and exchange, are all very similar, 0.27, 0.3 and 0.4 eV, respectively. Thus it is not surprising that they cannot be delineated in the conductivity data. The noteworthy point is that the activation energy for motion on the fast sub-lattice, 0.27 eV, is in agreement with the enthalpy for F^- vacancy migration determined from the conductivity, 0.28 eV. This suggests that at least the two techniques are monitoring the same process. It is not possible at the present time to make a

quantitative comparison of conductivity and N.M.R. The simple theories of evaluating diffusion coefficients from N.M.R. data, such as that developed by Torrey⁽³⁹⁾, assume a single mobile species and cannot account for LaF₃ where one F⁻ sub-lattice is static.

IV.3 The point defect structure and transport mechanisms in LaF₃

The early work of Sher et al⁽²⁶⁾ on the bulk and X-ray expansion of LaF₃ crystals has always been used as evidence of Schottky defects in LaF₃. The bulk expansion was significantly greater than the X-ray expansion. However, the activation energy for defect formation, Schottky quartet (1 La³⁺ vacancy + 3F⁻ vacancies), was anomalously low at 0.069 eV. The expansion experiments to determine defect concentrations are notoriously difficult. Although we have assumed in this report that the defects in LaF₃ are Schottky defects it is clearly far from certain. The alternative possibility is that the basic defects are of the anion-Frenkel type (F⁻ vacancy and F⁻ interstitial). Unfortunately, transport measurements alone cannot resolve this problem. The only way this can be resolved is by further expansion measurements or calculations of the defect energies using a computer simulation of the HADES type⁽⁶¹⁾.

The effect of assuming that the disorder would make relatively minor differences in the interpretation of our data. Clearly the crystals doped with M²⁺ or O²⁻ impurity would still contain predominantly vacancies and the enthalpies measured would still be for vacancy processes. The crystals doped with Th⁴⁺ would contain excess F⁻ interstitials and enthalpies would therefore relate to these defects. From a simple treatment of our data on an anion Frenkel model we would estimate the formation enthalpy to be 1.06 eV.

The defect structure of LaF₃ above 900K is expected to be anomalous. Recent heat capacity data⁽⁶²⁾ shows an anomalous increase

(61) Catlow, C.R.A., Norgett, M.J. and Ross, T.A., 1977, J.Phys.C: Solid State Phys., 10, 1627.

(62) Lyon, W.G., Osborne, D.W., Flotow, H.E. and Grandjean, F., 1978, J.Chem.Phys., 69, 167.

above 900K. A crude analysis suggests that LaF_3 contains - 10% defects at the melting point. This rise in heat capacity is similar to that observed in fluorites⁽⁶³⁾, except that in the latter case it decreases again before the melting point. If the heat capacity data is taken as being due to a spontaneous generation of defects then this could account for the data of Sher et al.

Although most workers have concluded that doping LaF_3 with M^{2+} creates F^- vacancies there are discrepancies in the interpretation of the conductivity data. The conductivity plots in the extrinsic region of M^{2+} doped LaF_2 are clearly curved, see Figure 12, with a high temperature activation energy of ~0.3 eV and a low temperature activation energy of ~0.4 - 0.5 eV. The problem is in the assignment of the origin of this curvature and hence the evaluation of the enthalpy of vacancy migration. There are three possible interpretations. Firstly, the curvature could be due to association of the F^- vacancies and M^{2+} at low temperatures and the subsequent loss of charge carriers. The second possibility is that the curvature is due to the motion of F^- vacancies occurring at different rates on different sublattices, i.e. the interpretation of the N.M.R. data. The final possibility is that the curvature is due to a combination of both these effects.

We have interpreted our conductivity data in terms of association. The computer fitting that we have employed is not really proof of this interpretation, however, it does show that the extrinsic region can be fitted by the sum of only two exponentials. We have favoured the interpretation using association since it must be present at low temperatures. In fact, we recently obtained information that confirms this beyond doubt. A dielectric study by Professor Fontanella (U.S. Naval Academy, Annapolis) detected a strong relaxation due to the

(63) Hayes, W., 1978, *Contemp.Phys.*, 19, 469.

reorientation of complexes. Thus association must be included in the interpretation of the conductivity data. Therefore, despite the criticism by Schoonman et al⁽⁵³⁾, we would stand by our original interpretation of the conductivity and our estimate of the F⁻ vacancy migration enthalpy of 0.28 eV.

On the model of Schottky disorder the effect of the Th⁴⁺ doping would be to create La³⁺ vacancies. If the disorder were anion Frenkel defects the excess defects would be F⁻ interstitials. Our data shows that whatever the defect is it has an enthalpy of migration of about 0.50 eV.

Our results for the conductivity anisotropy have been confirmed in the recent work of Schoonman et al⁽⁵³⁾. In some ways the result is surprising at first sight. It might have been expected that the conductivity within the closer-packed layer of the ab plane i.e. \perp to the c-axis would have been higher. However, it should be remembered that the measurements were taken in the extrinsic region, in fact, in a region where defect association is important. Thus we would conclude that the somewhat unusual result may be due to the different type of F⁻ site on which complexing can occur.

Our conductivity results for the heavy-doped LaF₃ with SrF₂ shows that these crystals are good F⁻ ion conductors. As we showed the earlier data of Nagle and O'Keeffe⁽²⁸⁾ for La_{0.95} Sr_{0.05} F_{2.95} were lower than our result, probably because they did not use crystalline samples. Takahashi et al⁽³¹⁾, having only the Nagle and O'Keeffe⁽²⁸⁾ data for comparison, came to the conclusion that Ce_{0.95} Ca_{0.05} F_{2.95} was a much better conductor than La_{0.95} C_{0.05} F_{2.95}. Our results show there is virtually no difference between the conductivity of the two materials.

Finally, the interpretation that we have developed for the N.M.R. results provides a good fit to the data. This model should be applicable to other systems with ions on non-equivalent sites.

V. CONCLUSIONS

This study of ionic conductivity and N.M.R. in tysonite fluorides is the most thorough study of transport in these materials that has been reported.

We have developed our own crystal growing facilities for the production of good samples of these materials and the results show the necessity of single crystals for reliable transport studies.

We have developed procedures for the quantitative interpretation of both the N.M.R. and the conductivity results.

On the basis of a Schottky model of point defect disorder we have evaluated the energies of defect formation and migration. We have also given a discussion of the effect on defect energies if it was assumed that the predominant point defects in tysonites were anion Frenkel defects.

The tysonites doped with divalent metal cations are good F^- ion conductors. We have shown that doped LaF_3 is as good a conductor as any of the other tysonite fluorides. Their use in battery systems would be governed more by the selection of suitable electrode systems than by the ionic conductivity of the systems.

VI. RECOMMENDATIONS FOR FUTURE WORK

The nature of the basic point defect structure in tysonite fluorides, Schottky or anion Frenkel, is still very much an open question. A problem that is coupled with this is the origin of the high temperature specific heat behaviour, which suggest the creation of a high concentration of defects. In an attempt to resolve these problems one of us (A.V.C.) will be involved with a neutron diffraction study of LaF_3 at the Institute Laue-Langevin in 1981.

The correlation of the conductivity and N.M.R. measurements has not been fully resolved in this project. The biggest problem is preparation of LaF_3 samples with a low paramagnetic impurity content. If this could be overcome then further N.M.R. work could be very fruitful. Also helpful in this respect would be more conductivity studies on oriented samples. In particular, some measure of the degree of anisotropy in the intrinsic region would be very useful.

Evidence for complexes formed by the association of dopants with F^- vacancies has been seen in the dielectric relaxation behaviour by Professor Fontanella (U.S. Naval Academy, Annapolis). Studies of these complexes and complexes formed on doping with M^{4+} impurities by dielectric or ionic thermocurrent techniques⁽³⁵⁾ would be useful. They would help in the interpretation of the conductivity and N.M.R. data and in the assignment of the basic defect structures. Professor Fontanella and one of us (A.V.C.) have initiated a joint project to study dielectric relaxation in depth in LaF_3 .

From the point of view of devices made with tysonite fluorides the effort would have to go into the investigation of compatible electrode systems.

The tysonite fluorides are fascinating systems from the academic viewpoint and no doubt will continue to attract interest in the future.

VII. PUBLICATIONS FROM THIS PROJECT

The following papers have been published.

1. N.M.R. and Conductivity Studies of Ionic Transport in LaF₃,
A.V. Chadwick, D.S. Hope, G. Jaroszkiewicz and J.H. Strange
in "Fast Ion Transport in Solids" editors Vashishta, Mundy and
Shenoy (North Holland, New York), p. 683, 1979.

2. ¹⁹F N.M.R. Studies of LaF₃,
G. Jaroszkiewicz and J.H. Strange,
Journal de Physique 41, C-6, 246 , 1980.

Papers are in preparation on the details of the N.M.R. analysis of
systems with non-equivalent sites and transport in doped tysonites.

VIII. REFERENCES

- (1) McGeehin, P. and Hooper, A., 1975, "Fast ion conduction: A materials review", Harwell Report, AERE-R8070.
- (2) Van Gool, W., 1973, (ed) "Fast ion transport in solids", (North-Holland, Amsterdam).
- (3) Huggins, R., 1975, in "Diffusion in solids - recent developments", ed. Nowick and Burton (Academic Press, New York), chapter 9, p.445.
- (4) Hooper, A., 1978, Contemp. Phys., 19, 147.
- (5) Hagenmuller, P. and van Gool, W., 1978, ed. "Solid Electrolytes; General principles, characterization, materials, applications" (Academic, New York).
- (6) Geller, S., 1977, ed. "Solid Electrolytes" Topics in Applied Physics, Volume 21 (Springer, Berlin).
- (7) Salamon, M.B., 1979, ed. "Physics of Superionic Conductors" Topics in Current Physics, Volume 15 (Springer, Berlin).
- (8) Mahan, G.D. and Roth, W.L., 1976, ed. "Proc. Int. Conf. on Fast Ion Conductors, Schenectady", (Plenum, New York).
- (9) Second International Conference on Solid Electrolytes, 7-21 September 1978, St. Andrews, Scotland (no published proceedings).
- (10) Vashista, P., Mundy, J.N. and Shenoy, G.K., 1979, ed. "Fast Ion Transport in Solids", (North-Holland, New York). Proceedings of International Conference held 21-25 May 1979 at Lake Geneva, Wisconsin, U.S.A.
- (11) Third International Conference on Solid Electrolytes, September 1980, Tokyo, Japan.
- (12) Owens, B.B., Oxley, J.E. and Sammells, A.F., 1977, in "Solid Electrolytes" ed. Geller (Springer, Berlin).
- (13) See articles in reference (10).
- (14) Armand, M.B., Chabagno, J.M. and Duclot, M.J., 1979, in "Fast Ion Transport in Solids" ed. Vashishta, Mundy and Shenoy (North-Holland, New York) p.131.
- (15) Lidiard, A.B., 1957, in "Handbuch der Physik", Volume XX ed. Flügge (Springer, Berlin), p.246.

- (16) Rice, M.J., 1973, in "*Fast ion transport in solids*", ed. van Gool (North-Holland, Amsterdam), p.263 and references therein.
- (17) Sato, H. and Kikuchi, R., 1971, *J.Chem.Phys.*, 55, 677 and 702.
- (18) Jaccucci, G. and Rahman, A., 1978, *J.Chem.Phys.*, 69, 4117.
- (19) Dixon, M. and Gillan, M.J., 1980, *J.Phys.C: Solid State Phys.* 13, 1901 and 1919.
- (20) De Leeuw, S.W., 1978, *Molec.Phys.*, 36, 103.
- (21) Figueroa, D.R., Chadwick, A.W. and Strange, J.H., 1978, *J. Phys.C: Solid State Phys.*, 11, 55.
- (22) Carr, V.M., Chadwick, A.V. and Saghafian, R., 1978, *J.Phys.C: Solid State Phys.*, 11, L637.
- (23) Gordon, R.E. and Strange, J.H., 1978, *J.Phys.C: Solid State Phys.*, 11, 3218.
- (24) Catlow, C.R.A., 1980, *Comments in Solid State Phys.* (in press).
- (25) Schoonman, J., 1980, *Solid State Ionics*, 1, 121.
- (26) Sher, A., Solomon, R., Lee, K. and Muller, M.W., 1966, *Phys. Rev.*, 144, 593.
- (27) Fielder, W.L., 1969, *NASA Technical Report D-5505*.
- (28) Nagle, L.E. and O'Keefe, M., 1973, in "*Fast ion transport in solids*", ed. van Gool (North-Holland, Amsterdam) p.165.
- (29) Goldman, M. and Shen, L., 1966, *Phys.Rev.*, 144, 321.
- (30) Lee, K. and Sher, A., 1965, *Phys.Rev.Letters*, 14, 1027.
- (31) Takahashi, T., Iwahara, H. and Ishikawa, T., 1977, *J. Electrochem.Soc.*, 124, 280.
- (32) Reau, J-M. and Portier, J., 1978, "*Solid Electrolytes*" ed. Hagemuller and van Gool (Academic, New York) p.313.
- (33) Brown, D., 1968, "*Halides of the Lanthanides and Actinides*", (Wiley-Interscience, London).

- (34) Roth, W.L. and Muller, O., 1974, "Study, selection and preparation of solid cationic conductors". Final report N74-26498 (NASA - CR-134610).
- (35) Corish, J. and Jacobs, P.W.M., 1973, in "Surface and defect properties of solids", Vol.II (The Chemical Society, London) p.160.
- (36) Marquardt, D.W., 1963, J.Soc.Ind.Appl.Math., 11, 431.
- (37) Abragam, A., The Principles of Nuclear Magnetism (The Clarendon Press, Oxford, England, 1961).
- (38) Look, D.C. and Lowe, I.J., 1966, J. Chem. Phys., 44, 2995.
- (39) Torrey, H.C., 1953, Phys. Rev., 92, 962.
- (40) Eisenstadt, M. and Redfield, A.G., 1963, Phys. Rev., 132, 635.
- (41) Sholl, C.A., 1974, J.Phys.C: Solid St. Phys., 7, 3378.
1975, J.Phys.C: Solid St. Phys., 8, 1737.
- (42) Wolf, D., 1974, Phys. Rev., 10, 2710.
- (43) Zalkin, A. et al., 1966, Inorg. Chem., 5, No.8, 1467.
- (44) Mansmann, M., 1964, Z. Anorg. Chem., 331, 98.
- (45) Jaroszkiewicz, G. and Strange, J.H. (to be published).
- (46) Stockbarger, D.C., 1936, Rev. Sci. Inst., 7, 133.
- (47) Carr, H.Y. and Purcell, E.M., 1954, Phys. Rev., 94, 630.
- (47a) See, for example, reference (23).
- (48) Carr, V.M., Chadwick, A.V. and Figueroa, D.R., 1976, J. Physique, 37, C7 - 337.
- (49) Solomon, R., Sher, A. and Muller, M.W., 1966, J. Appl. Phys., 37, 247.
- (50) Jaroszkiewicz, G. and Strange, J.H., 1979, Proceedings of the Third Europhysical Conference on Lattice Defects in Ionic Crystals, September, Canterbury, U.K. To be published in J. de Physique.
- (51) Lilly, A.C., LaRoy, B.C., Tiller, C.O. and Whiting, B., 1973, J. Electrochem. Soc., 120, 1673.
- (52) Tiller, C.O., Lilly, A.C. and LaRoy, B.C., 1973, Phys. Rev. B, 8, 4787.

- (53) Schoonman, J., Oversluizen, G. and Wapenaar, K.E.D., 1980, (preprint of paper submitted for publication).
- (54) Murin, J. at al., 1980, Sov. J. Appl. Chem., 53, 1474 (in Russian).
- (55) Fielder, W.L., 1966, NASA TN D - 3346.
- (56) Fielder, W.L., 1967, NASA TN D - 3816.
- (57) Kirkwood, F.G., 1980, Ph.D. Thesis, University of Kent.
- (58) Jacobs, P.W.M., 1980, private communication.
- (59) Shen, L., 1968, Phys. Rev., 172, 259.
- (60) Ildstad, E., Svare, I. and Fjeldy, T.A., 1977, Phys. Stat. Sol. (a) 43, K65.
- (61) Catlow, C.R.A., Norgett, M.J. and Ross, T.A., 1977, J. Phys. C: Solid State Phys., 10, 1627.
- (62) Lyon, W.G., Osborne, D.W., Flotow, H.E. and Grandjean, F., 1978, J. Chem. Phys., 69, 167.
- (63) Hayes, W., 1978, Contemp. Phys., 19, 469.

**DATE
TIME**